Skyrmions

(Dated: April 30, 2015)

Skyrmions are a class of solitons, which are both topologically stable, meaning that their vacuum manifold has a non-trivial π_3 homotopy group, and energetically stable, meaning that they are local minima of the field energy. The non-linear sigma model is an effective hadronic field theory, based on a triplet of pion fields, which is a low energy approximation to QCD. With the addition of the Skyrme term, this approximate model may be improved to yield skyrmion solutions. Further improvements to the model allow us to give the pion fields mass. By considering a 'spherically symmetric', energy-minimising skyrmion solution corresponding to a winding number of $B = 1$, we deduce that the skyrmion has a mass of $\sim 1\,\mathrm{GeV}$ and a RMS radius of $\sim 1\,\mathrm{fm}$. By imposing CPT symmetry on the theory, we require the addition of the Wess-Zumino term to the action. From a calculation of the Noether charge corresponding to the baryon number symmetry group, $U(1)_V$, we deduce that the baryon number corresponds to the winding number of the skyrmion, which suggests that skyrmions are the baryons of QCD. By canonically quantizing the rotation of the $B = 1$ skyrmion and imposing electromagnetic gauge, we deduce the spin, isospin and physical electric charge. This supports the hypothesis that skyrmions correspond to baryons, and we identify the skyrmions corresponding to the proton and the neutron. Extending the theory, we discuss how light nuclei, with $B < 7$, may be successfully modeled using the single rational map ansatz. We briefly review the complications that arise when modeling larger nuclei ($B \geq 7$) and show that certain higher-order skyrmions may be successfully constructed using geometric rational map ansätze based on the Skyrme crystal.

CONTENTS

PREFACE

The aim of this essay is to give an academic introduction to the Skyrme model in both a mathematical and physical context, focusing on its original applications to nuclear physics. Starting from a discussion of classical solitons, with a few prototypical examples, we go on to discuss the construction of the classical Skyrme model, quantize the theory and finally, review attempts that have been made to model larger nuclei. The order is logically progressive and is intended to provide motivation for further study.

I. INTRODUCTION

In the past century, there have been many developments in the field of nuclear physics, which have lead to our current understanding of the structure of the nucleus. Physics has progressed from a simple representation of nucleons as point particles, with effective potential interactions, to a complete description based on quarks and gluons; known as quantum chromodynamics (QCD). In 1961, British nuclear physicist T. H. R. Skyrme conjectured that the interior of the nucleus is dominated by a 'medium' formed of three pion fields [1, 2]. Remarkably, this conjecture predates the advent of QCD and so, may be regarded as an intermediary step towards the construction of the modern standard model. However, as it was later realised, the simple ideas of Skyrme have a far wider significance in many, seemingly disparate, areas of physics [3].

II. CLASSICAL SOLITONS

This subsection is based on the original paper by Russell [4].

Before we go on to explore the full theory of Skyrme, it is important to review a few basic concepts from classical physics. Let us begin our discussion by examining soliton

solutions in classical field theory.

The phenomenon of solitons was first documented in the early 19th century, albeit in a more lowly form. In 1834, Scottish civil engineer and navel architect, J. S. Russell, first reported the phenomenon while conducting experiments to improve the efficiency of canal boats on the Union Canal in Scotland [4]. Russell observed that when a canal boat was rapidly drawn along a narrow path and subsequently brought to a stop, a solitary wave of water propagated out in front of it. In his own words: "the mass of water in the channel which [the canal boat] had put in motion...rolled forward with great velocity, assuming the form of a large solitary elevation, a rounded, smooth and well-defined heap of water, which continued its course along the channel apparently without change of form or diminution of speed" [4]. Indeed, it was not the wave itself that was surprising but rather the unusual physical properties that it possessed; most notably, the fact that it maintained its shape and seemingly did not dissipate energy. Russell subsequently followed the wave on horseback for "one or two" miles before he lost it due to the windings of the canal. He later reproduced the wave in a wave tank that he had built at home and named it the "wave of translation" [4]. So fascinated was he in his newly discovered solitary wave of translation, that he studied it for many years conducting both theoretical and experimental research into its key properties. Using Russell's observations, let us informally define a soliton in the following way:

> **Definition:** A *soliton* is a wave-packet that maintains its shape while propagating at a constant velocity. Broadly speaking, solitons have three defining features:
>
> - They are of permanent form (i.e. static solutions of the field equations),
>
> - They are localised within a region (i.e. they have finite size and finite energy);
>
> - They can interact with other solitons, and emerge from the collision unchanged, except for a phase shift.

At the time, Russell's ideas were hard for the scientific community to accept because they appeared to contradict the well-tested laws of hydrodynamics presented by respected scientists, such as Newton [5] and Bernoulli [6]. In 1878, Lord Rayleigh published a paper to Philosophical Magazine supporting Russell's observations with mathematical theory [7]. What Russell had named a "wave of translation" was, in fact, a solution to a weakly non-linear dispersive partial differential equation (PDE), where the non-linear and dispersive effects had been canceled in the medium. This explanation was generally well-received by the community [8] and Russell's solitary wave has been studied in the field of fluid dynamics ever since.

However, it was not until the late 20th century, that the far-reaching consequences of Russell's observations were beginning to be unearthed. Thanks to the capabilities of modern computer simulations, solitons have rapidly found applicability to various fields of science and they currently form their own field of research.

FIG. 1. A simple pendulum hanging freely in a uniform gravitational field of strength g. The set-up consists of a light, rigid rod of length l fixed at one end to a frictionless pivot and inclined at an angle ϕ to the vertical. A bob of mass m and negligible size is attached to the other end of the rod. [9]
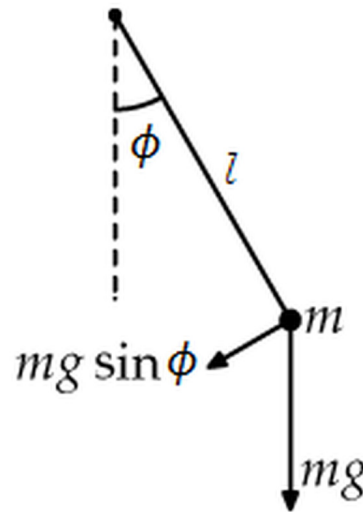
A. The Sine-Gordon Model

In order to introduce the analysis of classical solitons, let us start by examining the simple pendulum. Consider a simple pendulum of mass m, length l, and inclination angle ϕ, moving freely under gravity; as shown in figure 1. From this, we can write down the Lagrangian of the system as

$$L = \frac{1}{2}ml^2\dot{\phi}^2 - mgl(1 - \cos\phi), \qquad (1)$$

where $\dot{\phi} \equiv \mathrm{d}\phi/\mathrm{d}t$ denotes the time derivative. For simplicity, let us define a set of units in which all of the constants (i.e. m, g and l) are equal to one. This allows us to write the Lagrangian as

$$L = \frac{1}{2}\dot{\phi}^2 - (1 - \cos\phi). \qquad (2)$$

This is a classical simple harmonic oscillator with respect to the *scalar variable* $\phi(t)$. Now, by extending this concept to an infinite series of coupled harmonic oscillators, we can construct a field theory.

1. 1+1 dimensions

This subsection is based on lecture notes by Demokritov [10].

Imagine an infinite series of these simple, rigid pendula hanging from an infinitely long support rod, which extends from $x \to -\infty$ to $x \to \infty$, as shown in figure 2. Additionally, let each of the bobs of the pendula be coupled to their nearest neighbours by some coupling constant. For example, we may imagine they are coupled by elastic bands. Now, if we rotate one pendulum at $x \to -\infty$ completely

FIG. 2. A section of an infinite series of simple pendula hanging freely along the x-axis. [11]

FIG. 3. A propagating solitary wave of rotating pendula due to the non-zero coupling constant and the complete rotation of the pendulum at $x \to -\infty$ by an angle of $\phi_{x \to -\infty} = 2\pi$. [12]
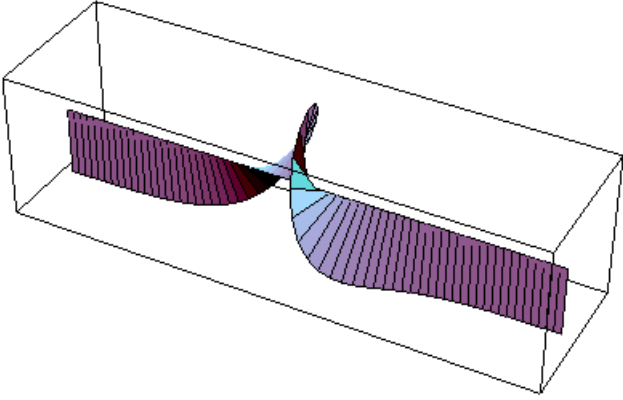
(i.e. by $\phi_{x \to -\infty} = 2\pi$), then since the pendula are coupled, this will send a solitary wave of rotating pendula propagating with a constant velocity in the positive x-direction, as illustrated in figure 3.

The Lagrangian for each pendulum may be parameterised by a scalar variable. Let us call this scalar variable the angle $\phi_n(t)$ for oscillator n. Since we have an infinite number of scalar variables, we may parameterise the Lagrangian of the system by the *scalar field* $\phi(t, x)$. Hence, working in Minkowski space with the usual particle physics metric $\eta^{\mu\nu} = \text{diag}(+1, -1, -1, -1)$, we may write the Lagrangian density of the system as

$$\mathcal{L} = \frac{1}{2}(\dot{\phi}^2 - \phi_x^2) - (1 - \cos \phi), \qquad (3)$$

where $\phi_x \equiv \partial \phi / \partial x$ and the Lagrangian may be recovered in the usual way, $L = \int_{-\infty}^{\infty} \mathcal{L} \, \mathrm{d}x$. Note that here we have simply moved from a scalar variable to a scalar field and from the time derivative factor, $\partial_t \phi \partial_t \phi$, in equation 2 to the space-time derivative factor, $\eta^{\mu\nu} \partial_\mu \phi \partial_\nu \phi$, with $c \stackrel{!}{=} 1$. For simplicity, natural units will be assumed for the continuation of this essay. Equation 3 gives us a relativistic theory and ensures that our scalar field is Lorentz invariant. Using Einstein notation, we may write this in a more

familiar and general form as

$$\mathcal{L} = \frac{1}{2}\partial_\mu \phi \, \partial^\mu \phi - V(\phi), \qquad (4)$$

where the effective potential $V(\phi) = 1 - \cos \phi \geq 0$. Now using the Euler-Lagrange equations,

$$\frac{\partial \mathcal{L}}{\partial \phi} - \partial_\mu \left(\frac{\partial \mathcal{L}}{\partial(\partial_\mu \phi)} \right) = 0, \qquad (5)$$

we may derive the equation of motion for ϕ to be

$$\boxed{\partial^2 \phi + \sin \phi = 0,} \qquad (6)$$

where $\partial^2 \equiv \partial^\mu \partial_\mu$ denotes the d'Alembert operator. This is known as the *sine-Gordon equation* and was originally used to study surfaces of constant negative curvature in geometry [13]. Nowadays, however, it has attracted a lot of interest due to its soliton solutions. The name "sine-Gordon" is a reference to its similarity with the well-known Klein-Gordon equation in quantum field theory. In fact, by writing the cosine as a Taylor series, the sine-Gordon Lagrangian density, $\mathcal{L}$, may be written as the Klein-Gordon Lagrangian density, $\mathcal{L}_{\text{KG}}$, plus higher-order terms:

$$\mathcal{L} = \underbrace{\frac{1}{2}\partial_\mu \phi \, \partial^\mu \phi + \frac{1}{2}\phi^2}_{\mathcal{L}_{\text{KG}}} + \sum_{n=2}^{\infty} \frac{(-\phi^2)^n}{(2n)!}. \qquad (7)$$

Now that we have our Lagrangian and equation of motion for our 1+1-dimensional scalar field theory, let us examine its key properties. First, note that the potential, $V(\phi)$, is minimised for all values $\phi = 2\pi k$, $k \in \mathbb{Z}$. Furthermore, since our system has a global symmetry $\phi \to \phi + 2\pi k$, we may choose the physical vacuum to be $\phi(x) \equiv 0$, without loss of generality. In our pendulum model, this corresponds to all of the pendula hanging downwards.

Now, suppose we have a soliton in our system. We know that solitons have a finite size and energy and so the pendula must be hanging downwards at $|x| \to \infty$. We do not know exactly what is happening in-between but at least the boundaries are clear:

$$\begin{cases} \phi(x \to -\infty) = 0 & (+2\pi k) \\ \phi(x \to +\infty) = 2\pi n & (+2\pi k), \end{cases} \qquad (8)$$

where we have defined the *winding number*

$$n \equiv \frac{\phi(\infty) - \phi(-\infty)}{2\pi} \in \mathbb{Z}. \qquad (9)$$

In other words, after we have created this soliton at $x \to -\infty$, we may reset the phase at $x \to -\infty$ to zero, as an arbitrary choice, and then the phase at $x \to \infty$ will be $2\pi n$, where n is the number of times we have wound the first pendulum to create the solitary wave. The whole system of course has a global symmetry of $\phi \to \phi + 2\pi k$ and so, strictly speaking, this term could also be present. However, we are only concerned with *relative* phases here and so we can ignore the global symmetry.

In order to have a closer look at the dynamics of the system, we can now solve the sine-Gordon equation of motion. Since solitons are "of permanent form" and move

at a constant velocity, we may solve the static (i.e. time-independent) sine-Gordon equation with the argument that we can always Lorentz boost to a frame where the soliton is stationary. In this case, from equation 6, the static sine-Gordon equation takes the form:

$$-\phi_{xx} + \sin\phi = 0. \tag{10}$$

Note that our angle of inclination ϕ is now just a function of x and so we have moved to straight derivatives in the equation. This leaves us with a simple 2nd-order differential equation that can be solved analytically. Multiplying through by ϕ_x yields

$$\phi_x \phi_{xx} = \phi_x \sin\phi; \tag{11}$$

which after integration becomes

$$\frac{1}{2}\phi_x^2 = -\cos\phi + A, \tag{12}$$

where A is a constant of integration. Noting that we are looking for solutions where $\phi, \phi_x \to 0$ as $|x| \to \infty$, we can deduce that $A = 1$. Using the trigonometric double-angle identity $\cos 2\phi \equiv 1 - \sin\phi$, we may rewrite this equation in terms of a sine function and integrate such that

$$\int_0^\phi \frac{d\phi}{\sin\frac{\phi}{2}} = \pm 2 \int_{x_0}^x dx, \tag{13}$$

where x_0 is the position of our soliton. Performing the integrals yields

$$\ln\left(\tan\frac{\phi}{4}\right) = \pm(x - x_0), \tag{14}$$

which we may subsequently rearrange to give us the final form of our solution:

$$\phi(x) = 4\arctan\left(e^{\pm(x-x_0)}\right). \tag{15}$$

Note that the $\pm$ in the exponent corresponds to a winding number of $n = \pm 1$, where the $n = +1$ case is called the *kink* solution and the $n = -1$, the *antikink*. A graph of these solutions is shown in figure 4. The kink may also be viewed as a non-dissipative (sech^2) wave-packet of energy moving along the x-axis, as shown in figure 5. This demonstrates how the phase and energy propagate through our system. Before we leave this example behind and move onto more complex systems, however, let us first examine two important properties of the kink soliton that will come in useful in later examples; namely its *mass* and its *size*. In our definition, we have stated that solitons are "localised within a region", meaning that they have finite energy and finite size. This being the case, it must be possible to compute these values.

The total mass of the soliton (or equivalently, the total energy, in this static configuration) may be computed by simply integrating over the Hamiltonian density. However, since we are considering the static case and are using the $(+---)$ metric convention, this is equivalent to integrating over minus the Lagrangian density. The energy functional is then given by

$$E[\phi] = \int_{-\infty}^\infty (-\mathcal{L})\,dx = \int_{-\infty}^\infty \left[\frac{1}{2}(\phi_x)^2 + V[\phi]\right]dx. \tag{16}$$

FIG. 4. The phase, ϕ, along the x-axis in the vicinity of a $|n| = 1$ soliton. The $n = +1$ case corresponds to the *kink* solution and the $n = -1$ case to the *antikink*. The soliton is centred at x_0 with a total length $2d$. [14]
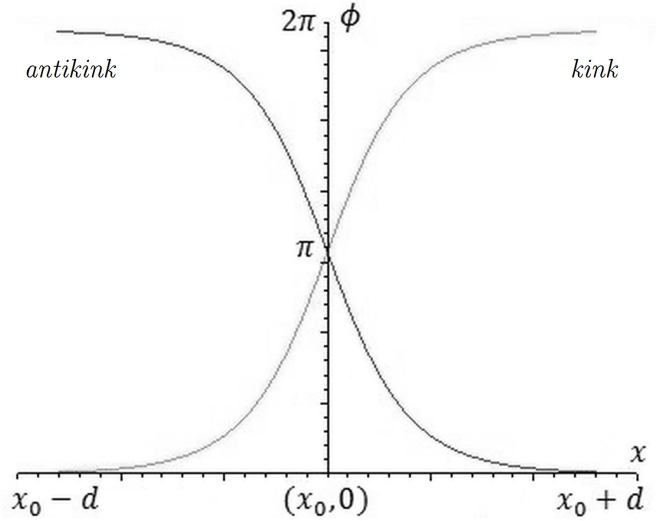
FIG. 5. The energy density, $\mathcal{E}$, along the x-axis in the vicinity of a $|n| = 1$ soliton. The soliton is centred at x_0 with a total length $2d$. [15]
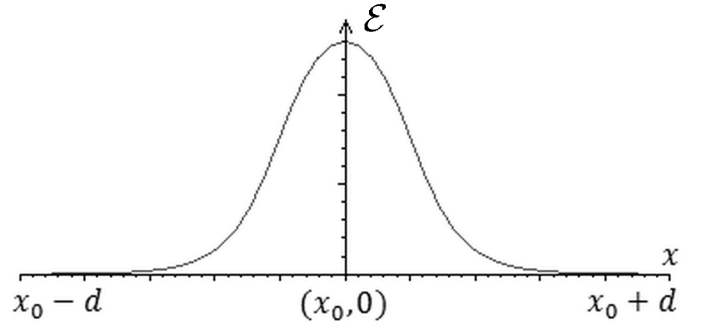
Calculating the x-derivative of our kink solution in equation 15 yields

$$\phi_x = \frac{4}{1 + e^{2(x-x_0)}} = \frac{4}{e^{x-x_0} + e^{-(x-x_0)}}, \tag{17}$$

which in terms of hyperbolic trigonometric functions reads

$$\phi_x = 2\,\text{sech}(x - x_0). \tag{18}$$

This gives us a kinetic energy density of

$$\frac{1}{2}(\phi_x)^2 = 2\,\text{sech}^2(x - x_0). \tag{19}$$

Following on from this and substituting the kink solution from equation 15 into our form of the effective potential yields

$$V(x) = 1 - \cos\left(4\arctan(e^{x-x_0})\right), \tag{20}$$

where the functional $V[\phi]$ has been reduced to a simple function of x. Using the cosine double-angle identity

$\cos 2\phi \equiv 1 - 2\sin^2\phi$ yields

$$V(x) = 2\sin^2\left(2\arctan(e^{x-x_0})\right), \qquad (21)$$

which after the application of the sine double-angle identity, $\sin 2\phi \equiv 2\sin\phi\cos\phi$, reduces to

$$V(x) = 8\sin^2\left(\arctan(e^{x-x_0})\right)\cos^2\left(\arctan(e^{x-x_0})\right). \quad (22)$$

From the arctangent functions in the expression, we can conclude that the ratio of opposite to adjacent sides of the right-angled triangle is e^{x-x_0}. Hence, using Pythagoras' theorem, this expression may be rewritten, in terms of hyperbolic trigonometric functions, as

$$V(x) = 2\operatorname{sech}^2(x - x_0). \qquad (23)$$

Comparing this to equation 19 shows that the kinetic and potential energies of our system are equal, which is what we would expect from Virial's theorem. Using these expressions, we may now perform the integral in equation 16 to find the total energy carried by our kink solution:

$$E[\phi_{n=+1}] = 4\int_{-\infty}^{\infty}\operatorname{sech}^2(x-x_0)\,\mathrm{d}x = 8. \qquad (24)$$

Note that due to the symmetry of the cosh function, this is also the energy carried by the antikink. Although it does not make much sense to talk about the 'mass' of the soliton in this context, the concept will come in useful later.

Last of all, we need an estimate for the soliton's size. We can compute this by considering the root-mean-squared (RMS) radius, $r_{\mathrm{RMS}} \equiv \sqrt{\langle r^2 \rangle}$, of the soliton's energy wavepacket. Following on from our discussion of the mass, the mean-squared radius can be calculated as

$$\langle r^2 \rangle \equiv \int_{-\infty}^{\infty}(x-x_0)^2(-\mathcal{L})\,\mathrm{d}x, \qquad (25)$$

which after a simple change of variables, defining $u \equiv x - x_0$, may be evaluated to give

$$r_{\mathrm{RMS}} = \left[4\int_{-\infty}^{\infty} u^2\operatorname{sech}^2 u\,\mathrm{d}u\right]^{1/2} = \sqrt{\frac{2}{3}}\pi. \qquad (26)$$

This gives us a value for the RMS radius of the soliton and hence, a rough estimate of its size, which will be useful for comparing solitons in future discussions.

The crucial point to realise is that solitons are a direct consequence of a new vacuum of our theory (i.e. a new state of lowest possible energy). Recall that we chose the physical vacuum of our system to correspond to all pendula hanging downwards (i.e. $\phi(x) = 0$, $\forall x$). As soon as we create a soliton, this configuration can never be reached, since we will have a propagating wave that is traveling along an infinitely long x-axis. Hence, in this situation, our system is said to have a new *non-trivial* vacuum - non-trivial meaning that it is topologically distinct from the physical vacuum. This non-trivial vacuum gives rise to solitons which are finite in mass and size, and, most importantly, *cannot* decay because they do not have the same topological properties as the physical vacuum.

2. 3+1 dimensions

This subsection is based on the chapter "A Planar Skyrme-Like Model" by Cova [16].

In our 1+1-dimensional model, we saw how our soliton can essentially be viewed as a particle, of fixed mass and size, propagating along the x-axis. If we now move to 2+1 dimensions, with the condition that $\partial_y\phi = 0$ in the sine-Gordon equation of motion, our soliton can be regarded as a line propagating in the x-direction. By extension, in 3+1 dimensions, with the conditions that $\partial_y\phi = \partial_z\phi = 0$, our soliton solution represents a propagating domain wall moving in the x-direction. This propagating domain wall separates the region in front of it, which still has the physical vacuum of $\phi = 0$, and the region behind it, which has a new vacuum of $\phi = 2\pi$ and no way of naturally decaying back into the physical vacuum. Hence, we say that the vacuum manifold, $\mathcal{M}$, is a *disconnected space* given by

$$\mathcal{M} = \{\phi : V(\phi) = 1 - \cos\phi \overset{!}{=} 0\} \qquad (27)$$

and hence isomorphic to the set of all integers,

$$\mathcal{M} = \{\ldots, -4\pi, -2\pi, 0, 2\pi, 4\pi, \ldots\} \cong \mathbb{Z}. \qquad (28)$$

Note that the physical vacuum manifold, $\mathcal{M}_{\mathrm{phys}}$, is given by

$$\mathcal{M}_{\mathrm{phys}} = \{\phi : \phi = 0\} = 0, \qquad (29)$$

and so is topologically distinct from $\mathcal{M}$. The physical vacuum is trivial, as it is just a number, whereas the soliton vacuum manifold is non-trivial, as it can take many different values. The observation that solitons do not decay is therefore equivalent to the statement that the set of all integers cannot be mapped onto a point. Although this level of mathematical abstraction may seem unnecessary at the moment, it will prove to be crucial for understanding higher-order solitons in section II C.

B. Homotopy Groups

This subsection is based on the chapter "Topology in Field Theory" in Manton & Sutcliffe [17].

Now that we have seen why a non-trivial vacuum manifold topology is a necessary condition for the existence of solitons, we need a precise way of categorising manifold topologies. Supposing we have a field theory with a given vacuum manifold topology, once we have a way of categorising whether the vacuum topology is non-trivial, we will be able to say whether soliton solutions could potentially exist. For this purpose, we shall use *homotopy theory*.

Let X and Y be two unbounded manifolds and let us consider the continuous maps between them, $\Psi : X \to Y$. For example, Y could represent the vacuum manifold of our field theory. We now need to define what it means for such a map to be homotopic to another; or equivalently, in the same homotopy class.

TABLE I. Overview of the key features of the most common n-spheres.

n-sphere	Description
S^0	antipodal points
S^1	circle - $U(1)$ manifold
S^2	'ordinary' sphere
S^3	4-dimensional sphere - $SU(2)$ manifold

> **Definition:** A continuous map $\Psi_0 : X \to Y$ is said to be in the same *homotopy class* as another map $\Psi_1 : X \to Y$ if Ψ_0 can be continuously deformed into Ψ_1. Formally speaking, Ψ_0 is homotopic to Ψ_1 if there exists a continuous map $\tilde{\Psi} : X \times [0, 1] \to Y$ where a 'time' τ parameterises the interval, such that $\tilde{\Psi}|_{\tau=0} = \Psi_0$ corresponds to the 'initial' map and $\tilde{\Psi}|_{\tau=1} = \Psi_1$ to the 'final' map.

It is the concept of continuous deformations that is crucial to this definition.

We can extend this analysis if we consider the homotopy classes of continuous maps from the n-sphere:

$$\Psi : S^n \to Y. \tag{30}$$

Recall that the unit n-sphere is the defined as the set of points in $\mathbb{R}^{n+1}$ at unit distance from the origin. The most common n-spheres are given in table I. The homotopy classes of continuous maps from the n-sphere are special because one can define the composition of any two of these classes and show that the usual group axioms of closure, associativity, identity and inversion are satisfied. Hence, from these homotopy classes, one can construct homotopy groups.

> **Definition:** The set of homotopy classes of the continuous maps $\Psi : S^n \to Y$, $n \geq 1$ is known as the nth *homotopy group*, $\pi_n(Y)$.

Clearly the ability to sort homotopy classes into homotopy groups will be very useful in categorising topologies. However, we first need to justify why it is valid for us to use these n-sphere maps in place of our general maps from X to Y. As suggested before, let us suppose that we have a field theory with some vacuum manifold Y. We now want to look at the continuous map from X to Y. In order to make use of the n-sphere map in our analysis, we need to show that our X manifold is isomorphic to an n-sphere. It is easy to confirm that this requirement is satisfied, if we consider *stereographic projection*. For example, consider a 3-dimensional, infinite, continuous manifold $\mathbb{R}^3$. In this case, $\mathbb{R}^3$ can be identified with S^3 by a stereographic projection from the north pole $\mathbf{p}$, as shown in figure 6. Considering an infinite 3-sphere, we can see that by projecting from the north pole of this sphere to a tangential plane with respect to its south pole, we can recover all of $\mathbb{R}^3$ apart from the point corresponding to the pole itself. In other words, there is a one-to-one correspondence between $\{S^3 - \mathbf{p}\}$ and $\mathbb{R}^3$, assuming that all points at infinity

FIG. 6. A pictorial representation of a stereographic projection from S^n to $\mathbb{R}^n$. The north pole of the n-sphere is labeled by the point $\mathbf{p}$. [17]
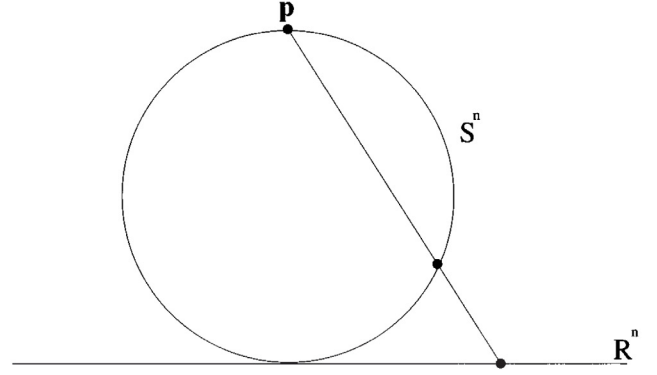
are identified. Now if we attach a point at infinity to $\mathbb{R}^3$, corresponding to the map of the pole, then we have our desired representation of S^3. This argument can trivially be extended to S^n.

Let us now build some intuition and learn how to exploit these homotopy groups. One of the simplest ways to get a feel for how these groups behave is to examine the homotopy groups of the m-sphere (i.e. considering maps from S^n to S^m). Let us start by examining the homotopy groups of the circle, S^1.

- $\pi_0(S^1) = 0$. This corresponds to mapping antipodal points onto a circle. Since any two points on S^1 are connected, there is only one topologically distinct way of putting antipodal points on a circle. Therefore, the target ('vacuum') manifold is trivial with respect to the 'initial' manifold, since it can only take one value. (Note also that we have not, strictly speaking, defined homotopy groups for $n = 0$. These are known as homotopy groups of *unbased* homotopy classes and need to be treated separately in a formal discussion [17].)

- $\pi_1(S^1) \cong \mathbb{Z}$. This corresponds to mapping a circle onto a circle. Note that here we are referring to a 'circle' in its topological sense, so it does not have to be round. In this case, we can deform a circle onto one side of the circumference of the target circle, which can correspond to method 0. Or, most obviously, we can put the circle on top of the other circle, which can correspond to method 1. Continuing in this vein, we can wrap around the target circle twice, which can correspond to method 2, etc. Remembering that we can wrap around the circle both clockwise and anti-clockwise implies that this homotopy group is isomorphic to the set of integers. In other words, there are an infinite number of topologically distinct ways of mapping a circle onto another circle. Hence, our target manifold is non-trivial with respect to the 'initial' manifold, since it can take multiple values.

Extending this to homotopy groups of the sphere S^2, we find that:

- $\pi_0(S^2) = 0$. This corresponds to mapping antipodal points onto a 2-sphere. As argued before, there is only one topologically distinct way of doing this, so the target manifold is trivial with respect to our original manifold.

- $\pi_1(S^2) = 0$. This corresponds to mapping a circle onto a 2-sphere. Any circle on a 2-sphere can be contracted to a point, or, in other words, there always exists a homeomorphism (continuous deformation) that can take a circle on a 2-sphere to a point on a 2-sphere. Therefore, on its surface, a circle and a point are topologically indistinguishable, and as we argued earlier, there is only one topologically distinct way of mapping a point onto a sphere. Hence, the target manifold is again trivial with respect to the original manifold.

- $\pi_2(S^2) \cong \mathbb{Z}$. This corresponds to mapping a 2-sphere onto another 2-sphere. Now this case is slightly more difficult to visualise but if we apply the same logic that we used for $\pi_1(S^1)$, we can conclude that the homotopy group is isomorphic to the set of all integers. Therefore, the target manifold is non-trivial with respect to the original manifold.

Anything beyond these simple cases quickly becomes very difficult to visualise, however as intuition may suggest, the general result is given by

$$\boxed{\pi_n(S^n) \cong \mathbb{Z}, \qquad \forall n \geq 1.} \tag{31}$$

However, note that the converse does not always hold: $\pi_n(S^m) \neq 0, \, \forall n \neq m$.

In this simple example, we have used homotopy theory to identify non-trivial target manifolds. Now, if we examine real vacuum manifolds of some field theory, then the homotopy groups will give us a way of checking if the manifold topology is non-trivial with respect to some 'initial' manifold. This gives us a way of identifying and classifying soliton solutions in a field theory.

C. Vacuum Manifold Topology

This subsection is based on the lectures by Gillioz [18].

From this point on, let us consider a 3+1-dimensional field theory with some vacuum manifold, $\mathcal{M}$ (e.g. the 3+1-dimensional sine-Gordon theory discussed in section II A 2). Calculating the homotopy groups of this manifold is simply an exercise in pure mathematics, as demonstrated in section II B. Therefore, let us proceed by interpreting what the first few non-trivial homotopy groups of the vacuum manifold will tell us about our field theory.

- $\pi_0(\mathcal{M}) \neq 0$. In this case, the vacuum manifold of our field theory is non-trivial with respect to the mapping of antipodal points. As we saw when we studied the homotopy classes of maps from S^n to S^m, there is only one topologically distinct way of mapping antipodal points onto a target manifold iff the antipodal points are connected on the target manifold. Consequently, in order for this $\pi_0(\mathcal{M})$ homotopy group to be non-trivial, our antipodal points must be disconnected when mapped onto the vacuum manifold. In other words, the antipodal points must be non-contractible (i.e. impossible to bring together) or equivalently, we must not be able to rotate the antipodal points into one another. This implies that there must be some 2-dimensional 'wall' (or 'walls') separating the two points. In fact, in this case, we say that our field theory has the potential for topological solitons called *domain walls*. We saw an example of this in section II A 2.

- $\pi_1(\mathcal{M}) \neq 0$. Here, the vacuum manifold is non-trivial with respect to the mapping of a circle. Again, for this homotopy group to be non-trivial, there must be closed paths in space that cannot be contracted to a point. This implies that there must be some 1-dimensional 'string' (or 'strings') passing through the circle in our vacuum manifold to prevent it from contracting to a point. In this case, we say that our field theory has the potential for topological solitons called *strings*. The most famous example of this being the cosmic strings in the abelian Higgs model, which has a manifold $\mathcal{M} = U(1) \cong S^1$ and non-trivial homotopy group $\pi_1(\mathcal{M}) \cong \mathbb{Z}$.

- $\pi_2(\mathcal{M}) \neq 0$. This corresponds to a non-trivial vacuum manifold with respect to the mapping of a 2-sphere. Extending our previous argument, there only exists more than one topologically distinct way of mapping a 2-sphere onto a target manifold iff the map of the 2-sphere on the manifold is a non-trivial surface. In other words, the map of the 2-sphere must be non-contractible. This implies that there must be some 0-dimensional 'singularity' (or 'singularities') within the sphere to prevent it from trivially contracting to a point. In this case, we say that our field theory has the potential for topological solitons called *monopoles*. A typical example of this being the magnetic monopoles in the non-abelian Higgs model, which has a manifold $\mathcal{M} = SU(2)/U(1)$ and non-trivial homotopy group $\pi_2(\mathcal{M}) \cong \mathbb{Z}$.

- $\pi_3(\mathcal{M}) \neq 0$. For our last example, we go one step beyond what is easy for us to visualise. However, based on the previous three cases, we should start to see a pattern emerging. This homotopy group corresponds to mapping a 3-sphere onto a vacuum manifold. Now, 3-spheres are difficult to visualise because they are in four spatial dimensions. However, as shown in section II B, we can identify a 3-sphere with the 3-dimensional space $\mathbb{R}^3$ by stereographic projection. Hence, this homotopy group corresponds to a non-trivial map of $\mathbb{R}^3 \to \mathcal{M}$. In order for this map to be non-trivial, there must be more than one topologically distinct way of mapping $\mathbb{R}^3$ onto our vacuum. So, as our intuition tells us, there could be some soliton in our field theory that creates this non-trivial surface. In fact, in this case, we say that our field theory has the potential for topological solitons called

skyrmions. There are many examples of theories with skyrmions because they can potentially exist in any theory with a $SU(N)$, $N \geq 3$ vacuum symmetry, as we shall see later.

Notice that throughout this discussion we have identified the cases where these solitons *could potentially* exist. This is because a non-trivial vacuum manifold topology is a necessary but *insufficient* condition for their existence. A soliton solution, as opposed to a *topological soliton*, also needs to be a local minimum of the energy functional.

D. Derrick's Scaling

This subsection is based on the original paper by Derrick [19].

Let us now consider the most general, renormalisable scalar field theory in 3+1 dimensions. The Lagrangian density for a general scalar field theory is given by

$$\mathcal{L} = \frac{1}{2} \partial_\mu \phi \, \partial^\mu \phi - V(\phi), \tag{32}$$

where $V(\phi)$ is some general potential function. As we have seen before, the energy functional for a (static) soliton configuration may be written as $E[\phi] = \int d^3x \, (-\mathcal{L})$, using our $(+---)$ metric. Hence, the full expression for the energy functional reads

$$E[\phi] = \int d^3x \left[+\frac{1}{2} \partial_i \phi \, \partial_i \phi - V(\phi) \right]. \tag{33}$$

We know that an additional constraint on the existence of stable soliton solutions is that the soliton configuration must be a local minimum of the energy functional. Formally speaking, this implies that the energy functional must satisfy

$$\left. \frac{\delta E}{\delta \phi} \right|_{\phi = \phi_0} = 0 \quad \text{and} \quad \left. \frac{\delta^2 E}{\delta \phi^2} \right|_{\phi = \phi_0} > 0, \tag{34}$$

for some soliton field configuration $\phi_0(x)$. Let us now label this minimised energy functional,

$$E_0 \equiv E_0^{(1)} + E_0^{(2)}, \tag{35}$$

where $E_0^{(1)}$ is the kinetic energy and $E_0^{(2)}$ the potential energy of our field configuration.

Using the fact that maps to a local vacuum manifold are continuous, we can represent any field configuration, $\phi(x)$, as a rescaling of our soliton field configuration, $\phi_0(x)$. Let us introduce a scaling parameter λ and define a general field configuration as

$$\phi_\lambda(x) \equiv \phi_0(\lambda x). \tag{36}$$

Note that now our general field configuration corresponds to the soliton configuration when $\lambda = 1$. Hence, our new conditions for the existence of soliton solutions are

$$\left. \frac{dE_\lambda}{d\lambda} \right|_{\lambda=1} = 0 \quad \text{and} \quad \left. \frac{d^2 E_\lambda}{d\lambda^2} \right|_{\lambda=1} > 0, \tag{37}$$

where we have gone from functional derivatives to straight derivatives because λ is simply a parameter. Recalling that our expression for the parameterised energy reads

$$E_\lambda = \int d^3x \left[\frac{1}{2} \partial_i \phi_0(\lambda x) \, \partial_i \phi_0(\lambda x) - V(\phi_0(\lambda x)) \right], \tag{38}$$

we may perform the substitution $x \equiv \tilde{x}/\lambda$ to remove the λ-dependence in the ϕ_0 functions, such that

$$E_\lambda = \int \frac{d^3\tilde{x}}{\lambda^3} \left[\frac{\lambda^2}{2} \partial_i \phi_0(\tilde{x}) \, \partial_i \phi_0(\tilde{x}) - V(\phi_0(\tilde{x})) \right]. \tag{39}$$

This allows us to express the general parameterised energy functional in terms of the kinetic and potential energies of the soliton configuration:

$$E_\lambda = \frac{1}{\lambda} E_0^{(1)} + \frac{1}{\lambda^3} E_0^{(2)}. \tag{40}$$

Now imposing the conditions identified above,

$$\left. \frac{dE_\lambda}{d\lambda} \right|_{\lambda=1} = -E_0^{(1)} - 3E_0^{(2)} \overset{!}{=} 0, \tag{41}$$

which implies that

$$E_0^{(2)} = -\frac{1}{3} E_0^{(1)}. \tag{42}$$

We can then easily determine the nature of this turning point by substituting this relation into the second derivative. Upon substitution, we find that

$$\left. \frac{d^2 E_\lambda}{d\lambda^2} \right|_{\lambda=1} = 2E_0^{(1)} + 12E_0^{(2)} = -2E_0^{(1)} \leq 0. \tag{43}$$

Since the kinetic energy of the soliton field configuration is always greater than or equal to zero, $E_0^{(1)} \geq 0$, this shows that the soliton configuration in a renormalisable 3+1-dimensional field theory is, in fact, a local maximum in energy, and so solitons cannot exist. This is a special case of G. H. Derrick's scaling argument, which states that stationary, localised solutions to wave-type equations are unstable in three or more spatial dimensions. From section II A 2, however, we showed that we would expect a domain wall in a 3+1-dimensional sine-Gordon model. Notice that although a domain wall is a *topological* soliton, meaning that it has a non-trivial vacuum manifold topology, it is not a valid soliton, as we defined them in section II, because it is *not* of finite energy and finite size. Since most of our theories of interest will be in 3+1 dimensions, Derrick's scaling argument is something that we will need to take into account.

III. THE CLASSICAL SKYRMION

In the previous section, we reviewed the basics of classical solitons that we will now use to understand the Skyrme model. We started by looking at the sine-Gordon model, and showed how solitons arise in a simple classical field theory. Studying the properties of a soliton in this context then gave us some intuition for how to generalise the

concept. Following on from this, we introduced the notion of homotopy groups and showed that non-trivial vacuum manifolds can be identified and categorised using homotopy theory. Finally, we concluded that in order for soliton solutions to exist they need to both have non-trivial vacuum manifolds *and* be local minima of the field energy.

We have now reached a point where, given some field theory (i.e. Lagrangian) we can definitively say whether the theory has the potential for solitons, and we are even able to describe their topology. Let us now apply these ideas to particle physics.

A. The Non-linear Sigma Model

This subsection is based on the conference lecture by Farhi [20].

In 1960, M. Gell-Mann and M. Levy introduced the theory of a scalar field that takes on values in a non-linear manifold [21]. For historical reasons, this model is named after Gell-Mann & Levy's scalar field, Σ, which was based on the spin-0 meson, σ, that they were modeling; however, this name is arbitrary. As mentioned before, the non-linear sigma model (NLSM) is a precursor to modern-day QCD. It is an effective field theory, which is valid at long distances and is a good approximation to QCD, when modeling physics in which the quark structure is negligible. The NLSM can therefore be viewed as a basic hadronic field theory; the base field in the model naturally being the lightest hadron: the pion.

This seminal theory changed the way that physicists thought about the structure of the atom and it even predates the discovery of quarks. Now instead of thinking about fundamental particles as points, we can think of them as scalar fields. In the NLSM, these scalar fields are made up of fields corresponding to the three pions:

$$\begin{cases} \pi^+ & : u\bar{d}, \\ \pi^0 & : \frac{1}{\sqrt{2}}(u\bar{u} + d\bar{d}), \\ \pi^- & : d\bar{u}, \end{cases}$$

which were the lightest, most fundamental building blocks that people knew of, at the time. Just as with the full QCD picture that follows, we require that our theory has a global symmetry group $SU(2)_L \times SU(2)_R$, in order for it to represent hadrons made up of two quark flavours.

Let $U(x)$ be an $SU(2)$-valued field, such that at every point in space-time, x, we assign an $SU(2)$ matrix, $U(x)$. Note that, in general, we would consider an $SU(N_f)$-valued field, where N_f is number of quark flavours. Here we are modelling pion fields and so there are only two quark flavours, corresponding to the up (u) and the down (d) quarks.

Since $U(x)$ is an $SU(2)$ field made up of the three pion fields $\{\pi^a(x) : a = 1, 2, 3\}$, it may be written as

$$U(x) = \exp(i\pi^a(x)\sigma^a/f_\pi), \tag{44}$$

where f_π is a pion decay constant with dimensions of mass, which we introduce to ensure that the argument of the

exponent is dimensionless, and σ^a are the Pauli matrices:

$$\{\sigma^a\} = \left\{ \begin{pmatrix} 0 & 1 \\ 1 & 0 \end{pmatrix}, \begin{pmatrix} 0 & -i \\ i & 0 \end{pmatrix}, \begin{pmatrix} 1 & 0 \\ 0 & -1 \end{pmatrix} \right\}. \tag{45}$$

This is a standard result for any $SU(2)$-valued field and so, may be rewritten in a more insightful way.

Derivation: By Taylor expanding the exponent, we may split the field up into even and odd parts as follows:

$$\begin{aligned} e^{i\boldsymbol{\pi}\cdot\boldsymbol{\sigma}/f_\pi} &= \sum_{n=0}^{\infty} \frac{1}{n!} \left(\frac{i}{f_\pi} \boldsymbol{\pi}\cdot\boldsymbol{\sigma} \right)^n \\ &= \underbrace{\sum_{n=0}^{\infty} \frac{(i\boldsymbol{\pi}\cdot\boldsymbol{\sigma}/f_\pi)^{2n}}{(2n)!}}_{\text{even}} + \underbrace{\sum_{n=0}^{\infty} \frac{(i\boldsymbol{\pi}\cdot\boldsymbol{\sigma}/f_\pi)^{2n+1}}{(2n+1)!}}_{\text{odd}}. \end{aligned} \tag{46}$$

Now using the Pauli matrix identity $\sigma^a\sigma^b \equiv \delta^{ab} + i\epsilon^{abc}\sigma^c$, we can see that

$$\begin{aligned} \pi^a\sigma^a\pi^b\sigma^b &= \pi^a\pi^b\sigma^a\sigma^b \\ &= \pi^a\pi^b\delta^{ab} + i\pi^a\pi^b\epsilon^{abc}\sigma^c. \end{aligned} \tag{47}$$

The second term vanishes because $\pi^a\pi^b$ is symmetric in its indices, whereas ϵ^{abc} is antisymmetric in a and b. Equation 47 implies that

$$(\boldsymbol{\pi}\cdot\boldsymbol{\sigma})^2 = \pi^2 \, \mathbb{1}, \tag{48}$$

where $\pi \equiv |\boldsymbol{\pi}|$, and $\mathbb{1}$ is the 2×2 identity matrix, and, more generally, the identity operator. From this, we can conclude that

$$(i\boldsymbol{\pi}\cdot\boldsymbol{\sigma}/f_\pi)^2 = -(\pi/f_\pi)^2 \, \mathbb{1} \tag{49}$$

and hence

$$(i\boldsymbol{\pi}\cdot\boldsymbol{\sigma}/f_\pi)^{2n} = (-1)^n (\pi/f_\pi)^{2n} \, \mathbb{1}. \tag{50}$$

Consequently, for our odd summand,

$$(i\boldsymbol{\pi}\cdot\boldsymbol{\sigma}/f_\pi)^{2n+1} = i(-1)^n (\pi/f_\pi)^{2n+1} \, \hat{\boldsymbol{\pi}}\cdot\boldsymbol{\sigma}, \tag{51}$$

where $\hat{\boldsymbol{\pi}}$ is defined to be the unit vector $\hat{\boldsymbol{\pi}} \equiv \boldsymbol{\pi}/|\boldsymbol{\pi}|$. Using these two relations, we can now express our exponential as

$$\begin{aligned} e^{i\boldsymbol{\pi}\cdot\boldsymbol{\sigma}/f_\pi} &= \sum_{n=0}^{\infty} \frac{(-1)^n(\pi/f_\pi)^{2n}}{(2n)!} \, \mathbb{1} \\ &+ i\sum_{n=0}^{\infty} \frac{(-1)^n(\pi/f_\pi)^{2n+1}}{(2n+1)!} \, \hat{\boldsymbol{\pi}}\cdot\boldsymbol{\sigma}. \end{aligned} \tag{52}$$

Expressing this in terms of harmonic functions, we find that our field may be neatly written as

$$U(x) = \cos(\pi/f_\pi) \, \mathbb{1} + i\sin(\pi/f_\pi) \, \hat{\boldsymbol{\pi}}\cdot\boldsymbol{\sigma}. \tag{53}$$

In this form, the symmetries of the field are manifest. Now the simplest possible Lagrangian density that we can

construct for a renormalisable scalar field theory with a $SU(2)_L \times SU(2)_R$ global symmetry group is

$$\mathcal{L}_{\text{NLSM}} = \frac{f_\pi^2}{4} \text{tr}(\partial_\mu U \partial^\mu U^\dagger), \tag{54}$$

where the factor of $f_\pi^2/4$ is simply a normalisation constant. Using equation 53 gives us an easy way of expanding the Lagrangian. Recall that we are working with pion fields and so the π has a space-time dependence, whereas all other quantities are constant. Taking the derivative of equation 53 yields

$$\partial_\mu U = -\frac{\partial_\mu \pi}{f_\pi} \sin(\pi/f_\pi) \, \mathbb{1} + i \frac{\partial_\mu \pi}{f_\pi} \cos(\pi/f_\pi) \, \hat{\boldsymbol{\pi}} \cdot \boldsymbol{\sigma}. \tag{55}$$

Expanding the harmonic functions up to quadratic order, we find that $\sin x \approx x$ and $\cos x \approx 1 - x^2/2$ and hence

$$\partial_\mu U \approx -\frac{\pi \partial_\mu \pi}{f_\pi^2} \, \mathbb{1} + i \frac{\partial_\mu \pi}{f_\pi} \, \hat{\boldsymbol{\pi}} \cdot \boldsymbol{\sigma} - i \frac{\pi^2 \partial_\mu \pi}{2 f_\pi^3} \, \hat{\boldsymbol{\pi}} \cdot \boldsymbol{\sigma}. \tag{56}$$

Similarly, for the remaining factor in the trace,

$$\partial^\mu U^\dagger \approx -\frac{\pi \partial^\mu \pi}{f_\pi^2} \, \mathbb{1} - i \frac{\partial^\mu \pi}{f_\pi} \, \hat{\boldsymbol{\pi}} \cdot \boldsymbol{\sigma} + i \frac{\pi^2 \partial^\mu \pi}{2 f_\pi^3} \, \hat{\boldsymbol{\pi}} \cdot \boldsymbol{\sigma}, \tag{57}$$

since Pauli matrices are hermitian. Multiplying these two expressions (equations 56 and 57) together yields

$$\partial_\mu U \partial^\mu U^\dagger \approx \frac{\partial_\mu \boldsymbol{\pi} \partial^\mu \boldsymbol{\pi}}{f_\pi^2} \cdot \boldsymbol{\sigma}^2 + \frac{(\pi \partial_\mu \pi)(\pi \partial^\mu \pi)}{f_\pi^4} \, \mathbb{1} \\ - \frac{\pi^2 (\partial_\mu \boldsymbol{\pi} \partial^\mu \boldsymbol{\pi})}{f_\pi^4} \cdot \boldsymbol{\sigma}^2, \tag{58}$$

up to quartic order in the reciprocal decay constant. Recalling the identities $\text{tr}(\mathbb{1}) = 2$ and $\text{tr}(\boldsymbol{\sigma}^2) = 2$, then allows us to expand our Lagrangian density (equation 54) as

$$\mathcal{L}_{\text{NLSM}} = \frac{1}{2} \partial_\mu \boldsymbol{\pi} \partial^\mu \boldsymbol{\pi} \\ + \frac{1}{2 f_\pi^2} \left[(\boldsymbol{\pi} \partial_\mu \boldsymbol{\pi})^2 - \pi^2 (\partial_\mu \boldsymbol{\pi})^2 \right] + O\left(\frac{1}{f_\pi^4} \right). \tag{59}$$

This justifies our choice of normalisation constant and shows that only even powers of the decay constant survive. Hence, our chosen Lagrangian density is simply the usual Lagrangian density for a free pion field plus higher-order terms $\sim O(1/f_\pi^2)$.

The global $SU(2)_L \times SU(2)_R$ symmetry implies that our Lagrangian is symmetric under the transformation

$$U \to LUR^\dagger, \qquad L, R \in SU(2). \tag{60}$$

However, recalling that $UU^\dagger \equiv \mathbb{1}$, we can choose the vacuum state (without loss of generality) to be $\langle U \rangle = \mathbb{1}$, which breaks this symmetry down to the diagonal (vectorial) subgroup, $SU(2)_V$. In the vacuum state, our Lagrangian is now symmetric under

$$U \to VUV^\dagger, \qquad V \in SU(2). \tag{61}$$

The vacuum manifold is therefore given by the (axial) coset

$$\frac{SU(2)_L \times SU(2)_R}{SU(2)_V} \cong SU(2)_A. \tag{62}$$

If we now note that $SU(2)_A$ is isomorphic to $SO(3)$, we can identify the topology of our vacuum manifold. Since $SO(3)$ can be compactified onto S^3 by stereographic projection, we can use the results from section II B (and specifically, equation 31) to deduce that

$$\boxed{\pi_3(SU(2)_A) \cong \mathbb{Z}.} \tag{63}$$

We can think of this as the homotopy group of the broken symmetry or, alternatively, all the ways that one can nontrivially transform the vacuum. Note that $\pi_1(SU(2)_A) = \pi_2(SU(2)_A) = 0$ and so we do not expect to find any strings or monopoles. However, equation 63 implies that there may be skyrmions present in our pion field theory.

B. Topological Charge

In this subsection, we present an alternative way of identifying topological solitons: the non-zero winding number. Recall that in our discussion of the sine-Gordon kink, we attributed a winding number to our soliton (see equation 9). This number corresponded to how many times we wound a pendulum to produce our wave of translation. We can now generalise this idea to higher-dimensional space.

Consider any special unitary field, such as the $SU(2)$ field in the NLSM. Now we would like to construct a topological invariant in three spatial dimensions, so this will need to involve the 3-component Levi-Civita tensor. Moreover, we need to contract all the indices of the Levi-Civita tensor and so we need three derivatives, $\partial_i, \partial_j, \partial_k$. Since our field U is unitary, we can only have an equal number of Us and $U^\dagger$s, and because we want to output a number, we take the trace. Consequently, the only topologically invariant quantity that we can build for a special unitary field U in three spatial dimensions is given by

$$\mathcal{B} = \frac{1}{24\pi^2} \epsilon_{ijk} \text{tr}(U^\dagger \partial_i U \partial_j U^\dagger \partial_k U), \tag{64}$$

where the prefactor is simply a normalisation constant, as we shall see later. This quantity is known as the *topological charge density* and hence, the *topological charge* may be obtained by taking the integral $B = \int \mathrm{d}^3x \, \mathcal{B}$, such that

$$B[U] = \frac{1}{24\pi^2} \epsilon_{ijk} \int \mathrm{d}^3x \, \text{tr}(U^\dagger \partial_i U \partial_j U^\dagger \partial_k U) \in \mathbb{Z}. \tag{65}$$

This is also sometimes referred to as the *winding number integral* as it characterises the non-trivial topology of a field, and it only takes integer values. The reason for the label B will become apparent later. Let us now show three important properties of this integral.

1. $\underline{B[U^\dagger] = -B[U].}$ To show this, we start by writing

$$B[U^\dagger] = \frac{1}{24\pi^2} \epsilon_{ijk} \int \mathrm{d}^3x \, \text{tr}(U \partial_i U^\dagger \partial_j U \partial_k U^\dagger). \tag{66}$$

Now the fact that U is unitary, $UU^\dagger \equiv \mathbb{1}$, implies

$$\partial_\mu (UU^\dagger) = (\partial_\mu U)U^\dagger + U(\partial_\mu U^\dagger) = 0, \tag{67}$$

and hence

$$U(\partial_\mu U^\dagger) = -(\partial_\mu U)U^\dagger. \tag{68}$$

Using this relation in the trace, simplifies the argument down to

$$-(\partial_i U)\,\boxed{U^\dagger \partial_j U}\,\partial_k U^\dagger.$$

We can now use a similar identity for the second (shaded) derivative, $U^\dagger(\partial_\mu U) = -(\partial_\mu U^\dagger)U$, to yield

$$(\partial_i U)(\partial_j U^\dagger)\,\boxed{U\partial_k U^\dagger}.$$

Finally, applying our relation to the third (shaded) derivative gives

$$-(\partial_i U)(\partial_j U^\dagger)(\partial_k U)U^\dagger,$$

which after using the cyclic property of the trace leaves us with

$$-U^\dagger(\partial_i U)(\partial_j U^\dagger)(\partial_k U).$$

This shows that

$$\boxed{B[U^\dagger] = -B[U]} \tag{69}$$

and hence that the winding number integral is anti-hermitian in its argument.

2. $\underline{\delta B = 0}$ for any infinitesimal transformation of the field $\underline{U(x)}$. To show this we can first start with the equivalent form of our integral (using equation 69)

$$B = -\frac{1}{24\pi^2}\epsilon_{ijk}\int \mathrm{d}^3x\,\mathrm{tr}(U\partial_i U^\dagger \partial_j U \partial_k U^\dagger). \tag{70}$$

Now applying the functional derivative with respect to U, we find that

$$\frac{\delta B}{\delta U} = -\frac{1}{24\pi^2}\epsilon_{ijk}\int \mathrm{d}^3x\,\mathrm{tr}(\partial_i U^\dagger \partial_j U \partial_k U^\dagger). \tag{71}$$

Recall that our soliton needs to have a finite energy and so our fields at infinity must be equal to the vacuum, that is $U(|x| \to \infty) = \mathbb{1}$. So now when we integrate by parts in the trace, our boundary term will vanish and we find that

$$\frac{\delta B}{\delta U} = -\frac{1}{24\pi^2}\epsilon_{ijk}\int \mathrm{d}^3x \\ \mathrm{tr}\left(-U^\dagger(\partial_i\partial_j U\partial_k U^\dagger + \partial_j U\partial_i\partial_k U^\dagger)\right). \tag{72}$$

When the first term in the trace is multiplied by the Levi-Civita tensor it vanishes, because the first term is symmetric in i and j, whereas the Levi-Civita symbol is antisymmetric in i and j. Similarly for the second term in the trace, the Levi-Civita tensor is antisymmetric in i and k, whereas the second term is symmetric in i and k. Hence, both terms vanish and we conclude that

$$\boxed{\frac{\delta B}{\delta U} = 0.} \tag{73}$$

This shows that our winding number integral is indeed a topological invariant and so it will remain unchanged under any infinitesimal transformation of the field.

3. $\underline{B[U_1 U_2] = B[U_1] + B[U_2]}$. To show this we can start in the expected way, by simply writing down $B[U_1 U_2]$, which yields

$$B[U_1 U_2] = \frac{1}{24\pi^2}\epsilon_{ijk}\int \mathrm{d}^3x \\ \mathrm{tr}(U_2^\dagger U_1^\dagger \partial_i(U_1 U_2)\partial_j(U_2^\dagger U_1^\dagger)\partial_k(U_1 U_2)), \tag{74}$$

where we have used the identity $(U_1 U_2)^\dagger \equiv U_2^\dagger U_1^\dagger$. For clarity, let us only write out the argument of the trace in our calculations. Expanding this out yields

$$\begin{aligned}
&U_2^\dagger U_1^\dagger(\partial_i U_1)U_2(\partial_j U_2^\dagger)U_1^\dagger(\partial_k U_1)U_2 && \text{term 1}\\
+&U_2^\dagger U_1^\dagger(\partial_i U_1)U_2(\partial_j U_2^\dagger)U_1^\dagger\,\boxed{U_1(\partial_k U_2)} && \text{term 2}\\
+&\cancel{U_2^\dagger}U_1^\dagger(\partial_i U_1)\cancel{U_2}\cancel{U_2^\dagger}(\partial_j U_1^\dagger)(\partial_k U_1)\cancel{U_2} && B[U_1]\\
+&U_2^\dagger U_1^\dagger(\partial_i U_1)U_2 U_2^\dagger(\partial_j U_1^\dagger)U_1(\partial_k U_2) && \text{term 4}\\
+&U_2^\dagger U_1^\dagger\,\boxed{U_1(\partial_i U_2)(\partial_j U_2^\dagger)U_1^\dagger(\partial_k U_1)U_2} && \text{term 5}\\
+&U_2^\dagger \cancel{U_1^\dagger}U_1(\partial_i U_2)(\partial_j U_2^\dagger)\cancel{U_1^\dagger}U_1(\partial_k U_2) && B[U_2]\\
+&U_2^\dagger U_1^\dagger U_1(\partial_i U_2)U_2^\dagger(\partial_j U_1^\dagger)(\partial_k U_1)U_2 && \text{term 7}\\
+&U_2^\dagger U_1^\dagger U_1(\partial_i U_2)U_2^\dagger(\partial_j U_1^\dagger)\,\boxed{U_1(\partial_k U_2)}. && \text{term 8}
\end{aligned}$$

Here we have identified that due to the fact that our fields are unitary, along with the additive and cyclic properties of the trace, term 3 can be identified with $B[U_1]$ and term 6 to $B[U_2]$. Now using similar arguments to those in the previous proof, we may integrate by parts.

For example, if we integrate term 2 by parts, we know that the boundary term vanishes due to our boundary conditions, and the higher-order derivative terms from the Leibniz rule vanish when multiplied by the antisymmetric Levi-Civita tensor. Hence, by appropriate integration by parts, we can send the shaded factor in term 2 from $U_1(\partial_k U_2) \to -(\partial_k U_1)U_2$. Term 2 then exactly cancels term 1.

Using a similar argument in term 8, by appropriate integration by parts, we can send $U_1(\partial_k U_2) \to -(\partial_k U_1)U_2$ and hence this term cancels exactly with term 7.

Finally, in term 5 we can integrate by parts three times, which gives us an expression of the same form as term 4 as well as an overall minus sign and hence, these terms also cancel exactly.

Consequently, using the fact that the trace is additive in its argument, we conclude that

$$\boxed{B[U_1 U_2] = B[U_1] + B[U_2].} \tag{75}$$

This implies if we take the product of two fields, to form a new composite field, the winding numbers simply add. This is what we would intuitively expect if we took the product of two sine-Gordon fields.

FIG. 7. A graphical representation of the pion field configuration, $\boldsymbol{\pi} \in \mathbb{R}^3$. The magnitude of the vector arrows is directly proportional to the radial pion field function, $F(r)$. [22]
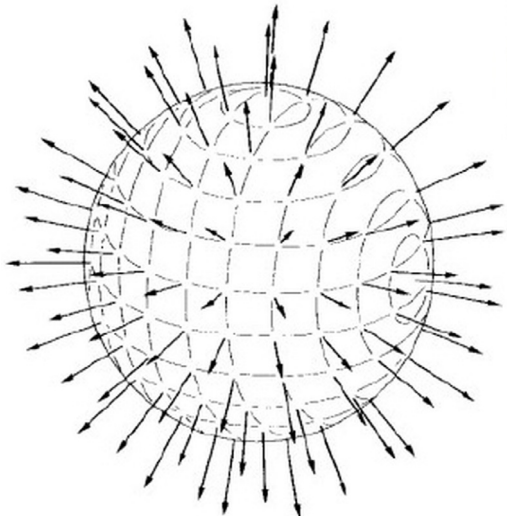
C.   The Hedgehog Ansatz

This subsection is based on the chapter "Skyrmions" in Manton & Sutcliffe [17], as well as discussions with Prof. Manton.

Now that we have our topological charge, B, it is natural to ask, in the context of our $SU(2)$-valued field in the NLSM: what field U will minimise B? Naturally, the vacuum state, $U = \mathbb{1}$, has zero winding number, $B(\mathbb{1}) = 0$, as we would expect. However, we are interested in what non-trivial field minimises the topological charge. For this, let us consider a 'spherically symmetric' field

$$U_{\mathrm{H}}(r) = \exp(iF(r)\hat{\boldsymbol{r}} \cdot \boldsymbol{\sigma}) \in SU(2), \qquad (76)$$

where $F(r)$ is an arbitrary function of r and $\hat{\boldsymbol{r}}$ is the radial unit vector in spherical polar coordinates. Looking back to equation 44, we can see that this ansatz corresponds to a pion field

$$\boldsymbol{\pi}(r) = f_\pi F(r)\hat{\boldsymbol{r}}. \qquad (77)$$

Hence this pion field is spherically symmetric and points radially outwards, as shown in figure 7. As such, this is commonly known as the *hedgehog ansatz*. It is now important to note the distinction between group space and position space. "Spherically symmetric" in this sense does not mean that the U field is merely a function of the radial coordinate, r. As we can see from equation 65, this sort of U field would give zero winding number. In this context, when we refer to 'spherical symmetry' we mean that the field has the equivariance property that a rotation in space is equivalent to a $SU(2)_V$ global transformation, which, as we saw earlier, is a symmetry of the Lagrangian (see equation 61).

We now need to look at the boundary conditions imposed on our pion field function, $F(r)$. As we have discussed before, our field configuration needs to have finite energy

and so the fields at infinity must tend to our vacuum state, which we chose to be $\langle U \rangle \equiv \mathbb{1}$. In terms of our hedgehog ansatz, this means that we need to impose the condition $U(|x| \to \infty) = \mathbb{1}$, which implies that

$$F(\infty) = 0. \qquad (78)$$

Furthermore, we require that our field is continuous everywhere. To check this condition, let us rewrite our hedgehog ansatz in terms of trigonometric functions, just as we did with the NLSM field configuration in section III A,

$$U_{\mathrm{H}}(r) = \cos F(r)\, \mathbb{1} + i \sin F(r)\, \hat{\boldsymbol{r}} \cdot \boldsymbol{\sigma}, \qquad (79)$$

where we note that $F(r)$ is actually the polar angle in group space. At the origin, our field cannot have any 'out-pointing' component, due to continuity. Therefore, our boundary condition must impose that $\sin F(0) = 0$, which implies

$$F(0) = n\pi, \qquad n \in \mathbb{Z}. \qquad (80)$$

Now that we have our boundary conditions for the hedgehog ansatz, we can substitute our expression for U_{H} (equation 79) into the winding number integral B (equation 65) and evaluate it. This is possible to do by brute force and recalling the identity $\sigma_i \sigma_j \equiv 2\delta_{ij} + i\epsilon_{ijk}\sigma_k$ [23, 24]. However, it will prove to be a good investment to think more deeply about the winding number.

Consider the winding number, as we first defined it in section II A 1, of the form

$$n = \frac{\phi(\infty) - \phi(-\infty)}{2\pi}. \qquad (81)$$

In this context it was very easy to visualise. It was simply the number of times that the soliton was 'wrapped' around the axis of propagation (i.e. the x-axis). The winding number was also intuitive to calculate and so we did not need to think too deeply about the formalism. In section III B, we generalised this concept by looking for a topological invariant for our field $U \in SU(2)$ in three spatial dimensions. Let us now formalise our method in a geometrical way, so that we may gain a greater insight into how the winding number is constructed.

In one spatial dimension, there is only one angle parameterising the winding number of our soliton. Let us regard this angle, Φ, as tracing a 1-sphere of arbitrary radius. Neglecting any constant contribution of a radius, the 2-dimensional volume form (i.e. area form) of our 1-sphere is

$$d\Omega^{S^1} = d\Phi. \qquad (82)$$

Now if we integrate this volume form over all space we find that

$$\int d\Omega^{S^1} = \int_0^{2\pi} d\Phi = 2\pi. \qquad (83)$$

Therefore, our normalised volume form may be written as

$$\widehat{d\Omega}^{S^1} = \frac{d\Phi}{2\pi}. \qquad (84)$$

Mapping our abstract space back onto our real space sends $\Phi \to \phi$, where ϕ is the azimuthal angle around the x-axis. Then integrating the pullback of our normalised volume form over the complete real space gives us the winding number,

$$n = \int_{\mathbb{R}^1} \widetilde{\widehat{\mathrm{d}\Omega}}^{S^1} = \int_{x \to -\infty}^{x \to \infty} \frac{\mathrm{d}\phi}{2\pi} = \frac{\phi(\infty) - \phi(-\infty)}{2\pi}. \quad (85)$$

Equipped with this formalism, let us now calculate the winding number for our hedgehog ansatz, $B[U_\mathrm{H}]$. Recall that our field theory is in three spatial dimensions and so our (static) hedgehog ansatz is in the real space $\mathbb{R}^3$. We can choose to parameterise this space with spherical polar coordinates so that it has a radius r and angles (θ, ϕ). However, our hedgehog ansatz also belongs to a higher-order (group) space, $SU(2)$. As we can see from the form of the hedgehog ansatz given in equation 79, F is the polar angle in group space. In other words, U_H is a map from the real space, $\mathbb{R}^3$, onto the target manifold, S^3, with arbitrary radius and parameterised by the angles (F, Θ, Φ). Just as the 1-dimensional winding number could be interpreted as the number of times we wound around a 1-dimensional line, the 3-dimensional winding number can be interpreted as the number of times we are winding around a 3-dimensional sphere (see [25] for a generalisation of this concept to arbitrary maps). Neglecting any constant contribution of a radius, the 4-dimensional volume form of a 3-sphere is given by

$$\mathrm{d}\Omega^{S^3} = \sin^2 F \sin \Theta \, \mathrm{d}F \wedge \mathrm{d}\Theta \wedge \mathrm{d}\Phi. \quad (86)$$

Integrating this volume form over all space gives

$$\int \mathrm{d}\Omega^{S^3} = \underbrace{\int_0^\pi \sin^2 F \, \mathrm{d}F}_{\pi/2} \underbrace{\int_0^\pi \sin \Theta \, \mathrm{d}\Theta}_{2} \underbrace{\int_0^{2\pi} \mathrm{d}\Phi}_{2\pi} = 2\pi^2, \quad (87)$$

and hence our normalised volume form is

$$\widehat{\mathrm{d}\Omega}^{S^3} = \frac{1}{2\pi^2} \sin^2 F \sin \Theta \, \mathrm{d}F \wedge \mathrm{d}\Theta \wedge \mathrm{d}\Phi. \quad (88)$$

Now our hedgehog ansatz specifies how to pullback this differential form onto our real space. The hedgehog ansatz specifies that

$$\begin{cases} F \to F(r) & \Rightarrow \mathrm{d}F = F'\mathrm{d}r \\ \Theta \to \theta \\ \Phi \to \phi. \end{cases} \quad (89)$$

Taking the pullback of our normalised volume form and integrating over all real space yields

$$\int_{\mathbb{R}^3} \widetilde{\widehat{\mathrm{d}\Omega}}^{S^3} = \frac{1}{2\pi^2} \int_\infty^0 F' \sin^2 F \, \mathrm{d}r \underbrace{\int_0^\pi \sin \theta \, \mathrm{d}\theta}_{2} \underbrace{\int_0^{2\pi} \mathrm{d}\phi}_{2\pi}, \quad (90)$$

where we have been careful with the limits of our integral over r. Note that because we integrated F between the limits of 0 and π in equation 87, due to our boundary conditions (equations 78 and 80), the limits with respect to r

must be from ∞ to 0. Hence, for the hedgehog ansatz, we may write the winding number as

$$B[U_\mathrm{H}] = -\frac{2}{\pi} \int_0^\infty \mathrm{d}r \, F' \sin^2 F. \quad (91)$$

Using the double-angle identity $\cos 2F \equiv 1 - 2 \sin^2 F$ then allows us to evaluate this integral. After some simplification, this becomes

$$B[U_\mathrm{H}] = \frac{1}{\pi} \left[\frac{1}{2} \sin 2F - F \right] \Big|_{r=0}^{r \to \infty} = n \in \mathbb{Z}. \quad (92)$$

This shows that in the hedgehog ansatz, our winding number is completely determined by the freedom that we have in choosing our boundary condition at the origin. Therefore, if we want a winding number of one, then all we have to do is impose $F(0) = \pi$. This is again analogous to the sine-Gordon model, where the winding number of our soliton corresponded completely to how many times we rotated the pendulum at the 'origin'.

Aside: We may generalise this concept further by considering the hedgehog map and non-linear elasticity theory. Recall that, as we have shown, the hedgehog ansatz is a map $U_\mathrm{H} : \mathbb{R}^3 \to S^3$. However, notice from equation 89 that certain coordinates are deformed under this mapping, such as the radial function F, and some are not, such as the angles (θ, ϕ). Let us now introduce a strain tensor D_{ij} to quantify the coordinate stretching deformation induced by this map [17]. The strain tensor may be defined in each point in real space as

$$D_{ij} = -\frac{1}{2}\mathrm{tr}\left((\partial_i U) U^\dagger (\partial_j U) U^\dagger \right). \quad (93)$$

This is a symmetric, positive-definite 3×3 matrix with eigenvalues λ_1, λ_2 and λ_3. For the hedgehog ansatz map, the strain matrix is written as

$$\mathbf{D} = \begin{pmatrix} \lambda_1 & 0 & 0 \\ 0 & \lambda_2 & 0 \\ 0 & 0 & \lambda_3 \end{pmatrix} = \begin{pmatrix} F' & 0 & 0 \\ 0 & \frac{\sin F}{r} & 0 \\ 0 & 0 & \frac{\sin F}{r} \end{pmatrix}. \quad (94)$$

Using the strain tensor, the topological charge, B, may be computed as the complete spatial integral of the topological charge density, $\mathcal{B}$, given by

$$\mathcal{B} = \frac{1}{2\pi^2} \lambda_1 \lambda_2 \lambda_3. \quad (95)$$

Note that the sign of λ_1, λ_2 and λ_3 are chosen such that $\lambda_1 \lambda_2 \lambda_3$ is positive (negative) if U is locally orientation preserving (reversing). In the case of the hedgehog ansatz, this gives

$$B[U_\mathrm{H}] = \frac{1}{2\pi^2} \int_\infty^0 F' \sin^2 F \, \mathrm{d}r \int_0^\pi \sin \theta \, \mathrm{d}\theta \int_0^{2\pi} \mathrm{d}\phi, \quad (96)$$

as before (cf. equation 90). Furthermore, using the strain tensor, we may also compute the energy density,

$\mathcal{E}$, which may be expressed as

$$\mathcal{E} = \frac{1}{12\pi^2}(\lambda_1^2 + \lambda_2^2 + \lambda_3^2 + \lambda_1^2\lambda_2^2 + \lambda_2^2\lambda_3^2 + \lambda_3^2\lambda_1^2). \quad (97)$$

Likewise, we can then find the (static) energy by taking the complete spatial integral, such that $E = \int \mathrm{d}^3x\,\mathcal{E}$.

D. Constructing the Skyrme Model

This subsection is based on the lectures by Gillioz [18], as well as the review by Zahed & Brown [26].

Recall that at the end of section III A, we concluded that because of the non-trivial topology of the NLSM, and specifically the non-trivial homotopy group $\pi_3(SU(2)_A)$, there may be skyrmions present in our theory. In the previous section, we looked at a particular 'spherically symmetric' field configuration that can be treated analytically. We again saw how it is possible for this field configuration to produce a non-zero winding number, indicating the potential for solitons. However, as discussed in section II D, the scaling argument of Derrick forbids the existence of solitons in this theory because due to our renormalisable, 3+1-dimensional scalar field Lagrangian density

$$\mathcal{L}_{\text{NLSM}} = \frac{f_\pi^2}{4}\mathrm{tr}(\partial_\mu U \partial^\mu U^\dagger), \quad (98)$$

the soliton configuration would be a local maximum of the field energy, and hence unstable. So, now we need to re-think the non-linear sigma model as Skyrme did in 1961 [1].

As mentioned in section III A, the NLSM is a hadronic field theory made up of a triplet of pion fields. It is an *effective* field theory, which is valid when modeling physics in which the quark structure is negligible. In other words, it is a low energy approximation to the true theory (QCD). Now at low energies, we know that terms in the Lagrangian with the lowest number of space-time derivatives will dominate. For the NLSM, we therefore chose a kinetic term with the fewest number of space-time derivatives that would still preserve the global $SU(2)_L \times SU(2)_R$ symmetry, which allows us to model chiral pions (i.e. two). However, at higher energies, terms with a higher number of space-time derivatives will become significant. In fact, the next higher-order terms that still satisfy the required global symmetry are terms with four derivatives, given by:

$$\begin{cases} \mathrm{tr}(\partial_\mu U \partial^\mu U^\dagger \partial_\nu U \partial^\nu U^\dagger), & \text{term 1} \\ \mathrm{tr}(\partial_\mu U \partial_\nu U^\dagger \partial^\mu U \partial^\nu U^\dagger), & \text{term 2} \\ \left[\mathrm{tr}(\partial_\mu U \partial^\mu U^\dagger)\right]^2, & \text{term 3} \\ \left[\mathrm{tr}(\partial_\mu U \partial_\nu U^\dagger)\right]^2. & \text{term 4} \end{cases}$$

However, in the case of QCD only two of these terms are linearly independent, as we can rewrite the double trace terms as:

$$\begin{cases} \left[\mathrm{tr}(\partial_\mu U \partial^\mu U^\dagger)\right]^2 \equiv 2\,\mathrm{tr}(\partial_\mu U \partial^\mu U^\dagger \partial_\nu U \partial^\nu U^\dagger), \\ \left[\mathrm{tr}(\partial_\mu U \partial_\nu U^\dagger)\right]^2 \equiv \mathrm{tr}(\partial_\mu U \partial^\mu U^\dagger \partial_\nu U \partial^\nu U^\dagger) \\ \qquad - \mathrm{tr}(\partial_\mu U \partial_\nu U^\dagger \partial^\mu U \partial^\nu U^\dagger). \end{cases} \quad (99)$$

Hence, only terms 1 and 2 are linearly independent. The choice of Skyrme was to add on one specific linear combination of terms 1 and 2 to the NLSM Lagrangian density, namely

$$\mathrm{tr}(\partial_\mu U \partial_\nu U^\dagger \partial^\mu U \partial^\nu U^\dagger) - \mathrm{tr}(\partial_\mu U \partial^\mu U^\dagger \partial_\nu U \partial^\nu U^\dagger),$$

which is simply term 2 minus term 1; or alternatively, minus term 4. Since the trace is additive in its argument, we combine these into a single trace with argument

$$\partial_\mu U \partial_\nu U^\dagger \partial^\mu U \partial^\nu U^\dagger - \partial_\mu U \partial^\mu U^\dagger \partial_\nu U \partial^\nu U^\dagger.$$

It is then possible to show that this argument is equivalent to

$$\frac{1}{2}[U^\dagger \partial_\mu U, U^\dagger \partial_\nu U][U^\dagger \partial^\mu U, U^\dagger \partial^\nu U],$$

where $[\cdot,\cdot]$ represents the commutator.

Check: Expanding these commutators out, neglecting the factor of $1/2$, leaves us with four terms:

$$U^\dagger(\partial_\mu U)U^\dagger(\partial_\nu U)U^\dagger(\partial^\mu U)U^\dagger(\partial^\nu U)$$
$$-U^\dagger(\partial_\mu U)U^\dagger(\partial_\nu U)U^\dagger(\partial^\nu U)U^\dagger(\partial^\mu U)$$
$$-U^\dagger(\partial_\nu U)U^\dagger(\partial_\mu U)U^\dagger(\partial^\mu U)U^\dagger(\partial^\nu U)$$
$$+U^\dagger(\partial_\nu U)U^\dagger(\partial_\mu U)U^\dagger(\partial^\nu U)U^\dagger(\partial^\mu U).$$

Now examining the first term more closely and applying the identity $U^\dagger(\partial_\mu U) = -(\partial_\mu U^\dagger)U$, allows to write

$$U^\dagger(\partial_\mu U)\underbrace{U^\dagger(\partial_\nu U)}_{-(\partial_\nu U^\dagger)U}\cancel{U^\dagger}(\partial^\mu U)\underbrace{U^\dagger(\partial^\nu U)}_{-(\partial^\nu U^\dagger)U}.$$

We can also see that because of the fact that the trace is additive in its argument and due its cyclic property, we can cycle the last U so that it cancels with the first $U^\dagger$. This leaves us with

$$\partial_\mu U \partial_\nu U^\dagger \partial^\mu U \partial^\nu U^\dagger,$$

which is of the correct form. Now let us examine the second term more closely, namely

$$-U^\dagger(\partial_\mu U)U^\dagger(\partial_\nu U)U^\dagger(\partial^\nu U)U^\dagger(\partial^\mu U).$$

Again using the additive and cyclic property of the trace, we can cycle this argument to

$$-(\partial^\mu U)U^\dagger(\partial_\mu U)U^\dagger(\partial_\nu U)U^\dagger(\partial^\nu U)U^\dagger.$$

We can now lower and raise the μ as per standard summation convention and then apply the identity $U^\dagger(\partial_\mu U) = -(\partial_\mu U^\dagger)U$, which yields

$$-(\partial_\mu U)\underbrace{U^\dagger(\partial^\mu U)}_{-(\partial^\mu U^\dagger)U}\cancel{U^\dagger}(\partial_\nu U)\underbrace{U^\dagger(\partial^\nu U)}_{-(\partial^\nu U^\dagger)U}\cancel{U^\dagger}.$$

Upon cancellations, this leaves us with

$$-\partial_\mu U \partial^\mu U^\dagger \partial_\nu U \partial^\nu U^\dagger,$$

which is also of the correct form. Repeating this process for the third and forth terms, we get exactly the same terms once more. Hence, accounting for the factor of $1/2$, we can see that our linear combination of traces may indeed be written as

$$
\begin{aligned}
&\operatorname{tr}(\partial_\mu U \partial_\nu U^\dagger \partial^\mu U \partial^\nu U^\dagger - \partial_\mu U \partial^\mu U^\dagger \partial_\nu U \partial^\nu U^\dagger) \\
&\equiv \frac{1}{2} \operatorname{tr}\left([U^\dagger \partial_\mu U, U^\dagger \partial_\nu U][U^\dagger \partial^\mu U, U^\dagger \partial^\nu U]\right),
\end{aligned}
\tag{100}
$$

which is the more common form in the literature.

Now, we can move from the NLSM to the Skyrme model with the addition of one extra term, known as the Skyrme term, $\mathcal{L}'_{\text{Skyrme}}$. Our Lagrangian density then becomes

$$
\mathcal{L}_{\text{Skyrme}} = \underbrace{\frac{f_\pi^2}{4}\operatorname{tr}(\partial_\mu U \partial^\mu U^\dagger)}_{\mathcal{L}_{\text{NLSM}}} + \underbrace{\frac{1}{32e^2}\operatorname{tr}[U^\dagger \partial_\mu U, U^\dagger \partial_\nu U]^2}_{\mathcal{L}'_{\text{Skyrme}}},
\tag{101}
$$

where e is a dimensionless Skyrme coupling parameter and the prefactor of $1/16$ simply ensures proper normalisation. In fact, the Skyrme term is the *unique* four derivative term that you can add to the NLSM Lagrangian, which both stabilises the energy of the skyrmion configuration and contains at most two time derivatives.

The fact that the Skyrme term stabilises the energy of the skyrmion configuration is crucial, as this is what motivated us to add on this additional term in the first place. It ensures that there is a lower bound on the mass of the skyrmion or, in other words, it means that the local minimum energy criterion is satisfied and because of the topology of the model (see section III A), there will be skyrmions in our field theory.

Furthermore, the Skyrme term contains at most two time derivatives because it is antisymmetric in its Lorentz indices. This is significant because it will allow us to canonically quantize the skyrmion and write down the usual conjugate momenta, as we shall see in section IV E.

Incidentally, the Skyrme term also happens to be the dominant term in the $1/N_c$ expansion of QCD; as confirmed by pion scattering data [18]. However, as mentioned before, the Skyrme model predates QCD and so this was not known to Skyrme at the time. Note that recently Skyrme models with higher-order derivative terms have also been studied, but are beyond the scope of this essay [27].

Let us now apply the scaling argument of Derrick to show that skyrmions do indeed exist in our field theory. We shall proceed, as in section II D, by considering the energy of a static field configuration in D dimensions:

$$
E[U] = \int \mathrm{d}^D x \left[+ \frac{f_\pi^2}{4}\operatorname{tr}(\partial_i U \partial_i U^\dagger) - \frac{1}{32e^2}\operatorname{tr}[U^\dagger \partial_i U, U^\dagger \partial_j U]^2 \right].
\tag{102}
$$

Note that here we are integrating minus the Lagrangian density. In the first term, the $(+---)$ metric was used when lowering the second index, which makes the term positive. In the second term, the metric does not need to be used and so, the term remains negative. Now suppose

that the energy functional has a turning point at $U = U_0$, such that

$$
\left.\frac{\delta E}{\delta U}\right|_{U=U_0} = 0,
\tag{103}
$$

where U_0 is the soliton field configuration under consideration. Using this, we can define our energy functional as a function of U_0, such that

$$
E_0 \equiv E_0^{(1)} + E_0^{(2)},
\tag{104}
$$

where

$$
\begin{cases}
E_0^{(1)} = \dfrac{f_\pi^2}{4} \displaystyle\int \mathrm{d}^D x \, \operatorname{tr}(\partial_i U_0 \partial_i U_0^\dagger), \\
E_0^{(2)} = -\dfrac{1}{32e^2} \displaystyle\int \mathrm{d}^D x \, \operatorname{tr}[U_0^\dagger \partial_i U_0, U_0^\dagger \partial_j U_0]^2.
\end{cases}
\tag{105}
$$

Now let us define a rescaled field, scaled by some parameter λ, such that

$$
U_\lambda(x) \equiv U_0(\lambda x),
\tag{106}
$$

where the $\lambda = 1$ case corresponds to our soliton field. In terms of our scaled field, the energy functional may be written as

$$
\begin{aligned}
E_\lambda = \int \mathrm{d}^D x \Bigg[&\frac{f_\pi^2}{4}\operatorname{tr}\left(\partial_i U_0(\lambda x)\partial_i U_0^\dagger(\lambda x)\right) \\
&- \frac{1}{32e^2}\operatorname{tr}[U_0^\dagger(\lambda x)\partial_i U_0(\lambda x), U_0^\dagger(\lambda x)\partial_j U_0(\lambda x)]^2 \Bigg].
\end{aligned}
\tag{107}
$$

Under the change of variables, $x \equiv \tilde{x}/\lambda$, we may write this integral in terms of our soliton field energies

$$
\begin{aligned}
E_\lambda = \int \frac{\mathrm{d}^D \tilde{x}}{\lambda^D} \Bigg[&\frac{f_\pi^2 \lambda^2}{4}\operatorname{tr}\left(\partial_i U_0(\tilde{x})\partial_i U_0^\dagger(\tilde{x})\right) \\
&- \frac{\lambda^4}{32e^2}\operatorname{tr}[U_0^\dagger(\tilde{x})\partial_i U_0(\tilde{x}), U_0^\dagger(\tilde{x})\partial_j U_0(\tilde{x})]^2 \Bigg],
\end{aligned}
\tag{108}
$$

which may be expressed as

$$
E_\lambda = \lambda^{2-D} E_0^{(1)} + \lambda^{4-D} E_0^{(2)}.
\tag{109}
$$

We know that, by definition, $\lambda = 1$ is a turning point and so

$$
\left.\frac{\mathrm{d}E_\lambda}{\mathrm{d}\lambda}\right|_{\lambda=1} = (2-D)E_0^{(1)} + (4-D)E_0^{(2)} \overset{!}{=} 0,
\tag{110}
$$

which implies that

$$
E_0^{(2)} = -\frac{2-D}{4-D} E_0^{(1)}.
\tag{111}
$$

If we check the nature of this turning point, we find that

$$
\left.\frac{\mathrm{d}^2 E_\lambda}{\mathrm{d}\lambda^2}\right|_{\lambda=1} = (2-D)(1-D)E_0^{(1)} + (4-D)(3-D)E_0^{(2)},
\tag{112}
$$

which after substitution of our result from equation 111, becomes

$$
\left.\frac{\mathrm{d}^2 E_\lambda}{\mathrm{d}\lambda^2}\right|_{\lambda=1} = 2(D-2)E_0^{(1)},
\tag{113}
$$

which is greater than zero, and therefore a local minimum, for all spatial dimensions $D \geq 3$:

$$2(D-2)E_0^{(1)} > 0, \qquad \forall D \geq 3. \tag{114}$$

Note, in particular, that for $D = 3$ we recover the Virial theorem as $E_0^{(1)} = E_0^{(2)}$ [26]. We will be working in $D = 3$ spatial dimensions and so, here we have shown that there will be skyrmions present in our field theory.

In fact, only using the information currently at our disposal, we can go even further and calculate a lower bound on the skyrmion energy. By rewriting our energy functional, using a method reminiscent of 'completing the square', for an operator K we can complete the $KK^\dagger$ to show that

$$E[U] = \int \mathrm{d}^3 x \left[\mathrm{tr}(KK^\dagger) \right. \\ \left. \mp \frac{f_\pi}{4e} \epsilon_{ijk} \mathrm{tr}(U^\dagger \partial_i U \partial_j U^\dagger \partial_k U) \right], \tag{115}$$

where

$$K \equiv \frac{f_\pi}{2} \partial_i U \pm \frac{1}{4e} \epsilon_{ijk} U \partial_j U^\dagger \partial_k U. \tag{116}$$

Now we know that the operator $KK^\dagger$ is a norm and so is clearly hermitian. We also know that hermitian operators always have positive eigenvalues and that the trace is simply the sum of all eigenvalues. Hence, we can conclude that $\mathrm{tr}(KK^\dagger) \geq 0$ and so

$$E[U] \geq \left| \frac{f_\pi}{4e} \epsilon_{ijk} \int \mathrm{d}^3 x \, \mathrm{tr}(U^\dagger \partial_i U \partial_j U^\dagger \partial_k U) \right|. \tag{117}$$

This inequality is known as the *Bogomolny bound*, although it was actually first introduced by Skyrme [18]. The integral should now look familiar. Indeed, it is of the same form as the winding number integral that we defined in equation 65. Identifying the winding number integral in the expression leads to

$$E[U] \geq 6\pi^2 \frac{f_\pi}{e} |B[U]|, \tag{118}$$

which now gives us a measurable lower bound on the skyrmion mass, M. For example, for the single ($B = 1$) skyrmion, the bound is given by

$$M_{B=1} \geq 6\pi^2 \frac{f_\pi}{e}. \tag{119}$$

Using approximate experimental values of $f_\pi \sim 100\,\mathrm{MeV}$ and $e \sim 5$ [28], we find that $M_{B=1} \gtrsim 1\,\mathrm{GeV}$. Note that unlike the Bogomolny bound in supersymmetry, this bound cannot be saturated and there are no BPS states, since we cannot choose a field such that $\partial_i U \propto \epsilon_{ijk} U \partial_j U^\dagger \partial_k U$ [18].

E.   Further Remarks

In the previous subsection, we saw how we could modify the, already topologically stable, NLSM to make it also energetically stable for soliton solutions, which in this case

happen to be skyrmions. We justified this modification to the Lagrangian and confirmed that the new Skyrme Lagrangian is indeed energetically stable using the scaling argument of Derrick. Finally, by completing the norm, or equivalently by the Cauchy-Schwartz inequality [26], we put a lower bound on our expected skyrmion mass. Let us now investigate what we can learn from this new model.

First of all, let us start by investigating the case of winding number magnitude one, $|B| = 1$. The simplest field that we can use to start our investigation is the 'spherically symmetric' hedgehog ansatz, U_H (equation 76). If we now substitute the hedgehog ansatz into the energy functional, or equivalently use the eigenvalues of the strain matrix as in equation 97, we obtain

$$E[U_\mathrm{H}] = 4\pi \frac{f_\pi}{e} \int_0^\infty \mathrm{d}r \\ \left[r^2 F'^2 + 2(\sin^2 F)(1 + F'^2) + \frac{\sin^4 F}{r^2} \right], \tag{120}$$

which is not solvable analytically when satisfying the boundary conditions $F(0) = \pi$, $F(\infty) = 0$, however may be evaluated numerically to give $M_\mathrm{H} \approx 72.9 f_\pi/e$ [17]. This energy is approximately 23% larger than the Bogomolny bound ($6\pi^2 f_\pi/e$). In fact, due to its 'spherical symmetry', the hedgehog ansatz is the lowest energy solution to the Skyrme Lagrangian for $|B| = 1$. Moreover, if we now evaluate the Euler-Lagrange equation

$$\frac{\delta E}{\delta F} = 0, \tag{121}$$

and use the double-angle identity $\sin 2F \equiv 2 \sin F \cos F$, then after some rearrangement we obtain the 2nd-order non-linear ordinary differential equation of motion

$$(r^2 + 2\sin^2 F)F'' + 2rF' + \sin 2F \left(F'^2 - 1 - \frac{\sin^2 F}{r^2} \right) = 0. \tag{122}$$

Unfortunately, this equation is again not solvable analytically whilst satisfying the boundary conditions, however it may be solved numerically (see [29] for a formal proof) to plot how our pion field function, F, evolves as a function of r; as shown in figure 8. As with the sine-Gordon model in section II A 1, we may now proceed in a similar way to calculate an estimate for the RMS radius of the skyrmion:

$$r_\mathrm{RMS} = \sqrt{\frac{\int \mathrm{d}^3 x \, r^2(-\mathcal{L}_\mathrm{Skyrme})}{\int \mathrm{d}^3 x \, (-\mathcal{L}_\mathrm{Skyrme})}} \approx 1.46 \frac{1}{f_\pi e}. \tag{123}$$

This is the RMS radius of the energy density wave-packet. Remembering the suppressed factor of $\hbar \approx 197\,\mathrm{MeV} \cdot \mathrm{fm}$, we find that the RMS radius is $\sim 1\,\mathrm{fm}$.

In its current form, the Skyrme Lagrangian describes a triplet of *massless* pion fields. As shown in equation 59, for small fluctuations in the field, the Lagrangian density may be expanded as

$$\mathcal{L}_\mathrm{Skyrme} = \frac{1}{2} \partial_\mu \boldsymbol{\pi} \partial^\mu \boldsymbol{\pi} + O(\boldsymbol{\pi}^4), \tag{124}$$

which gives the kinetic energy term for free pions. However, a more realistic effective Lagrangian would also include a

FIG. 8. A plot of the pion field function, F, against radius, r, for the $B = 1$ hedgehog soliton solution. The boundary conditions are satisfied, such that $F(0) = \pi$ and $F(\infty) = 0$. Note that at large r, F scales as $1/r^2$. [17]
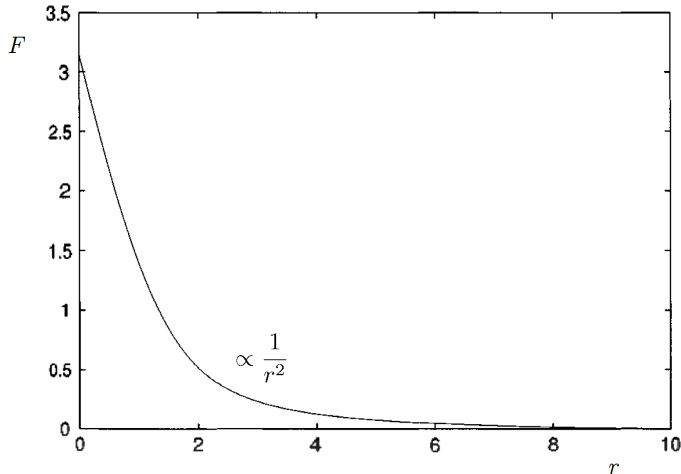
parity invariant, global symmetry breaking term that gives the pions mass, such that, for small fluctuations in the field, the Lagrangian density would be expanded as

$$\mathcal{L} = \frac{1}{2}\partial_\mu \boldsymbol{\pi}\partial^\mu \boldsymbol{\pi} - \frac{1}{2}m_\pi^2 \boldsymbol{\pi} \cdot \boldsymbol{\pi} + O(\boldsymbol{\pi}^4), \qquad (125)$$

where m_π is the introduced pion mass. Therefore, we need to add another term onto our Skyrme Lagrangian which will break the $SU(2)_L \times SU(2)_R$ global symmetry and give the pions a mass m_π. Recall that in a vacuum $U = \mathbb{1}$, there are no pions present and so our field theory should not have a mass. Therefore our additional mass term, $\mathcal{L}''_{\mathrm{mass}}$, must vanish when $U = \mathbb{1}$. The most general parity invariant term that we can write down satisfying these conditions is

$$\mathcal{L}''_{\mathrm{mass}} = \frac{m_\pi^2 f_\pi^2}{4}\mathrm{tr}(U + U^\dagger - 2\mathbb{1}), \qquad (126)$$

where, as with the NLSM, the factor of $f_\pi^2/4$ simply ensures proper normalisation. Hence, our improved total Lagrangian density, $\mathcal{L}$, may be written as

$$\boxed{\mathcal{L} = \mathcal{L}_{\mathrm{NLSM}} + \mathcal{L}'_{\mathrm{Skyrme}} + \mathcal{L}''_{\mathrm{mass}},} \qquad (127)$$

where $\mathcal{L}_{\mathrm{NLSM}}$ corresponds to the original NLSM Lagrangian density, $\mathcal{L}'_{\mathrm{Skyrme}}$ to the Skyrme term and $\mathcal{L}''_{\mathrm{mass}}$ to the pion mass term. This is the simplest effective field theory that successfully describes a triplet of massive pion fields with skyrmion solutions. As we have seen, the skyrmion in this theory is a massive ($\sim 1\,\mathrm{GeV}$), energetically and topologically stable structure with conserved quantum number, B. Skyrme made the bold assertion that this object is, in fact, a baryon with conserved *baryon number, B* [1]. We shall show this in more detail in section IV C. Now, we know that baryons are made up of three quarks and so, are fermions. However, mesons are made up of two quarks and so, are bosons. How can it be then, that an object which we have built out of bosons becomes a fermion?

E. Witten reconciled this issue in 1983, by realising that a skyrmion can be a fermion if the number of colours in the underlying theory is odd [30, 31]. The assertion made by Skyrme is therefore a remarkable result, which essentially states that baryons are the topological solitons (specifically, skyrmions) of a sigma model effective field theory. We shall discuss this in more detail in section IV D.

When discussing higher baryon numbers, it is important to note that the hedgehog ansatz is not generally the lowest energy solution to the Skyrme Lagrangian. For the more complicated cases of $B \geq 2$, we need to use the *rational map ansatz* instead [17, 32], which is beyond the scope of this essay. For example, for $B = 2$ we can use an axially symmetric ansatz to calculate the lowest energy $M_{B=2} \approx 140 f_\pi/e$, which is only slightly less than twice the computed value for the lowest energy $2M_{B=1} \approx 146 f_\pi/e$ [18]. Returning to our interpretation of these skyrmions as baryons, this observation could, for example, be used to explain why the binding energy of deuteron is so small [33]. Deuteron is made up of two baryons, a proton and a neutron, and it has a very small mass deficit as a composite particle when compared to the total mass of its constituents. Deuteron has baryon number 2 and so may be represented by $M_{B=2}$, whereas the proton and the neutron both have baryon number 1, which corresponds to $M_{B=1}$.

At the moment this is only a crude model, however we can see how we can quickly arrive at some interesting results. In order to make this effective model precise for these energies, we need to quantize the theory.

IV. SKYRMION QUANTIZATION

The conjecture that skyrmions may be interpreted as baryons in our Lagrangian is indeed a bold one, and one that needs more justification. As we now know, baryons are composite particles made up of three quarks. Quarks are fermionic particles of spin $1/2$ and so by extension, baryons must also be fermionic particles. Now for particles obeying Fermi-Dirac statistics, it is clear that quantum mechanics plays a significant role. Therefore, in order to obtain a full description of baryons, we need to quantize our theory. If the conjecture of Skyrme is correct, then upon quantization, we should be able to recover the other key details of the baryons under consideration, hence allowing us to identify them.

A. Lagrangian Symmetries

This subsection is based on the chapter "Skyrmions" in Manton & Sutcliffe [17].

We begin our discussion of skyrmion quantization in the natural way, by looking at the symmetries of our current total Lagrangian density,

$$\mathcal{L} = \frac{f_\pi^2}{4}\mathrm{tr}(\partial_\mu U \partial^\mu U^\dagger) + \frac{1}{32e^2}\mathrm{tr}[U^\dagger \partial_\mu U, U^\dagger \partial_\nu U]^2 \\ + \frac{m_\pi^2 f_\pi^2}{4}\mathrm{tr}(U + U^\dagger - 2\mathbb{1}). \qquad (128)$$

As we can see, there are three discrete symmetries obeyed by our Lagrangian and, in fact, by any Lagrangian made up of $SU(N_f)$-valued fields and their derivatives:

- Charge symmetry $C : U \to U^\dagger$. The NLSM term in our Lagrangian is clearly invariant under this symmetry, as we can simply swap the U and $U^\dagger$, use the cyclic property of the trace and raise and lower the μ indices, as per the standard summation convention.

  The charge symmetry in the Skyrme term is a little less obvious. Here we need to look at the original unsimplified form of our trace,

  $$\text{tr}(\partial_\mu U \partial_\nu U^\dagger \partial^\mu U \partial^\nu U^\dagger) - \text{tr}(\partial_\mu U \partial^\mu U^\dagger \partial_\nu U \partial^\nu U^\dagger).$$

  In the first trace, we can simply move from $U \to U^\dagger$ and then relabel $\mu \leftrightarrow \nu$. In the second trace, we can move from $U \to U^\dagger$ and then raise and lower the μ and ν index pairs. Hence, we can see that the Skyrme term is invariant under this symmetry.

  Finally, the pion mass term has a trivial charge symmetry and so our total Lagrangian is invariant under charge transformation.

- Parity symmetry $P : \mathbf{x} \to -\mathbf{x}$. Using our Minkowski metric $\eta^{\mu\nu}$ to contract the index in the first term, we can clearly see that, since our derivative terms always come in pairs, our Lagrangian is invariant under parity transformation.

- Time reversal symmetry $T : t \to -t$. Using similar reasoning for time reversal, we can see that because derivatives of the field always appear in pairs, the time transformation $t \to -t$ is negated and our Lagrangian is left unchanged.

Now, the fact that our Lagrangian obeys these three discrete symmetries is problematic. It is problematic because our Lagrangian should be a good description of natural processes (e.g. particle decays). However, natural processes do not obey C, P and T symmetries separately. Rather, natural processes obey CPT symmetry which is a simultaneous transformation. Therefore, for our Lagrangian to be an accurate description of nature, we first need to modify it so that it breaks the individual C, P and T symmetries, whilst still maintaining an overall CPT symmetry.

For this, let us examine the equations of motion of our total chiral Lagrangian. First we apply the Euler-Lagrange equations to our Lagrangian density (equation 128),

$$\frac{\partial \mathcal{L}}{\partial U} - \partial_\mu \left(\frac{\partial \mathcal{L}}{\partial (\partial_\mu U)} \right) = 0, \tag{129}$$

treat U and $U^\dagger$ as two independent fields, and ignore the constants brought up by the pion mass term. Note that for this subsection, we may ignore the pion mass term completely without loss of generality. Computing this, we find that $\partial \mathcal{L}/\partial U = 0$ and

$$\frac{\partial \mathcal{L}}{\partial U^\dagger} = (\partial_\mu U) U^\dagger (\partial_\nu U) + U^\dagger (\partial_\mu U)(\partial_\nu U)$$
$$- (\partial_\nu U) U^\dagger (\partial_\mu U) - U^\dagger (\partial_\nu U)(\partial_\mu U) = 0. \tag{130}$$

Consequently, our Euler-Lagrange equations reduce to

$$\partial_\mu \left(\frac{\partial \mathcal{L}}{\partial (\partial_\mu U)} \right) = 0. \tag{131}$$

This leaves our equation with five terms. After some rearrangement, they may be written more compactly as

$$\partial_\mu \left(-\frac{f_\pi^2}{2} (\partial_\mu U) U^\dagger \right.$$
$$\left. + \frac{1}{8e^2} \left[(\partial^\nu U) U^\dagger, [(\partial_\nu U) U^\dagger, (\partial^\mu U) U^\dagger] \right] \right) = 0. \tag{132}$$

Now we would like to introduce a breaking term (i.e. a term with a Levi-Civita tensor) that will break all of the individual symmetries that we have discussed but retain the overall CPT symmetry. This may be achieved quite simply by adding on a term with a 4-dimensional Levi-Civita tensor, of the form

$$\epsilon_{\mu\nu\rho\sigma} \partial^\mu U^\dagger \partial^\nu U \partial^\rho U^\dagger \partial^\sigma U.$$

Here the Levi-Civita tensor ensures that all of the individual symmetries are broken and this is the simplest possible term that we can write to contract all of the indices on the 4-component ϵ. As we can see, the overall CPT invariance remains in tact. At first glance, this would seem like a perfect choice for our correction term in the equation of motion. However, there is one significant problem: there is no possible *4-dimensional* term that we can add to the action that would produce this term upon variation.

B. The Wess-Zumino Term

This subsection is based on the review by Zahed & Brown [26].

J. Wess and B. Zumino reconciled this problem in 1971 by moving to five dimensions [34]. They proposed adding a new 5-dimensional term to the Skyrme action, now known as the Wess-Zumino correction, S_{WZ}, such that our new action may be written as

$$S = \left(\int \mathrm{d}^4 x \, \mathcal{L}_{\text{Skyrme}} \right) \pm S_{\text{WZ}}, \tag{133}$$

where $S_{\text{WZ}} \equiv \alpha \Gamma$, α is a factor to be determined (first introduced by Witten in 1983 [31]), and the sign ambiguity is eliminated in our equation of motion by the use of Stokes' theorem [26]. Here the Wess-Zumino term, Γ, is given by

$$\Gamma = -\frac{i}{240\pi^2} \int_{\mathcal{M}_5} \mathrm{d}^5 x$$
$$\epsilon^{\mu\nu\rho\sigma\tau} \text{tr}(U^\dagger \partial_\mu U \partial_\nu U^\dagger \partial_\rho U \partial_\sigma U^\dagger \partial_\tau U), \tag{134}$$

where the prefactor of $-i/240\pi^2$ simply ensures proper normalisation and $\mathcal{M}_5$ is an arbitrary 5-dimensional manifold which has the usual 4-dimensional Minkowski space as its boundary, $\partial \mathcal{M}_5 = \mathcal{M}_4$. Note that since the integrand of

the Wess-Zumino term may be identified with a curl, we can use Stokes' theorem to show that

$$\pm\Gamma = \mp \frac{i}{240\pi^2} \int_{\mathcal{M}_5} \mathrm{d}^5 x$$
$$\epsilon^{\mu\nu\rho\sigma\tau}\mathrm{tr}(U^\dagger\partial_\mu U\partial_\nu U^\dagger\partial_\rho U\partial_\sigma U^\dagger\partial_\tau U)$$
$$= -\frac{i}{240\pi^2} \int_{\partial\mathcal{M}_5} \mathrm{d}\mathbf{\Sigma}_\tau$$
$$\epsilon^{\mu\nu\rho\sigma\tau}\mathrm{tr}(U^\dagger\partial_\mu U\partial_\nu U^\dagger\partial_\rho U\partial_\sigma U^\dagger U), \tag{135}$$

where $\mathbf{\Sigma}$ is a space-time vector along the boundary of our 5-dimensional bulk, $\mathcal{M}_4$. From this we can see that, upon variation of the action, we will be able to obtain a term proportional to the one that is required in our equation of motion. Note that by the use of Stokes' theorem, our equation of motion will be in 4-dimensional physical space. Indeed, this 5-dimensional bulk that we have introduced is merely a mathematical trick and so, it should not affect the physics. In other words, our *path integral* must be independent of the choice of $\mathcal{M}_5$. Now as we know, the integrand of a path integral is of the form e^{iS}, where S is the action. Consequently, we can conclude that the path integral is invariant under multiple changes of 2π in the action. In order for our choice of $\mathcal{M}_5$ to not affect the physics, we therefore require that the change in the action under the shift $\mathcal{M}_5 \to \mathcal{M}_5{}'$ leaves the path integral invariant. This implies

$$\alpha\Gamma(\mathcal{M}_5) - \alpha\Gamma(\mathcal{M}_5{}') = 2\pi k, \qquad k \in \mathbb{Z}, \tag{136}$$

which, topologically, means that

$$\alpha\Gamma(\mathcal{M}_5 \cup \mathcal{M}_5{}') = 2\pi k, \qquad k \in \mathbb{Z}. \tag{137}$$

Without loss of generality, we may choose our $\mathcal{M}_5 \cup \mathcal{M}_5{}'$ to form a 5-ball in our $SU(N_f)$ manifold. In our normalisation, this means that $\Gamma(\mathcal{M}_5 \cup \mathcal{M}_5{}') = 2\pi$ and hence our factor α is an integer, $\alpha \in \mathbb{Z}$. In other words, mapping our 5-sphere onto a group, $S^5 \to G$, implies that our factor α is an integer provided G is a connected compact, simple Lie group. From this topological ambiguity argument, we can see why the factor of $\alpha \in \mathbb{Z}$ is needed. Witten showed that this factor is needed and that it can only take integer values in 1983 [31] [35]. However, we have yet to identify the role of α in our particle physics interpretation of skyrmions.

C. Baryon Number

This subsection is based on the lectures by Gillioz [18].

In the previous subsection, we showed why the choice of manifold $\mathcal{M}_5$ does not affect the physics of our system provided $\alpha \in \mathbb{Z}$. More generally, we require that the Wess-Zumino correction does not alter the physics of our system. Recall that the motivation behind adding this extra term was to fix the symmetries of our equation of motion. Therefore, we do not want our additional term to interfere with our general model. We can check that the correction term, S_{WZ}, does not affect the physics by looking at Noether currents associated with vector and axial transformations for

$U \to e^{(i\epsilon Q)}Ue^{-(i\epsilon Q)}$, which yields

$$\begin{cases} \delta_V U = i\epsilon[Q,U], \\ \delta_A U = i\epsilon\{Q,U\}, \end{cases} \tag{138}$$

respectively, where ϵ denotes a rotation parameter and Q denotes the global charge generator. Imposing electromagnetic gauge (see [36] for details), we find that the 4-dimensional Noether current associated with the Wess-Zumino correction may be written as

$$J^\mu_{V/A}(Q) = \frac{\alpha}{48\pi^2}\epsilon^{\mu\nu\rho\sigma}\Big[\mathrm{tr}(QU^\dagger\partial_\nu U\partial_\rho U^\dagger\partial_\sigma U)$$
$$\mp\mathrm{tr}(QU\partial_\nu U^\dagger\partial_\rho U\partial_\sigma U^\dagger)\Big]. \tag{139}$$

From this we can see that the traces vanish for any $SU(N_f)$ charge generator and hence, the additional correction term does not have any associated Noether currents and does not alter the physics of our system [18].

Let us now have a look at baryon number. Since baryon number symmetry corresponds to a $U(1)_V$ symmetry in our theory, this implies that $\delta_V U = 0$. Hence, to investigate baryon number further, we need to look at the case where $Q = \mathbb{1}$ in our Noether current in equation 139. Imposing this symmetry, only the vectorial Noether current survives. Let us denote this current as the *baryon current*, J_B. After some rearrangement, this may be written as

$$J^\mu_B = \frac{\alpha b}{24\pi^2}\epsilon^{\mu\nu\rho\sigma}\mathrm{tr}(U^\dagger\partial_\nu U\partial_\rho U^\dagger\partial_\sigma U), \tag{140}$$

where we have included the factor b, which is the baryon charge of a single quark, as we have not yet integrated over the triplet of fields. Noether's theorem states that under this continuous baryon number symmetry the baryon current and the associated *baryon charge* are conserved. As per Noether's theorem, the actual baryon charge, Q_B, may then be written as

$$Q_B = \int \mathrm{d}^3 x\, J^0_B$$
$$= b \int \mathrm{d}^3 x\, \epsilon^{ijk}\mathrm{tr}(U^\dagger\partial_i U\partial_j U^\dagger\partial_k U). \tag{141}$$

Again, this integral looks familiar as it is simply the winding number integral or baryon number, B, which we introduced in section III B. Therefore, the baryon charge may be written simply as

$$Q_B = \alpha b B. \tag{142}$$

We have suggested that the winding number integral may be interpreted as the baryon number of our theory, and we know from the $U(1)_V$ symmetry of baryon number, together with Noether's theorem, that Q_B must correspond to baryon charge, and b to the baryon charge of an individual quark. However, we do not yet have a physical interpretation for α, which could potentially confirm or refute the idea of viewing B as the baryon number.

With the advent of QCD, we can find an interpretation for this integer. By matching the anomalies of our infra-red theory (i.e. chiral action + Wess-Zumino correction) to the

anomalies of the QCD ultra-violet theory (i.e. quark model with $SU(N_c)$ gauge), we find that $\alpha = N_c$, where N_c is the number of quark colours. Then, by identifying the baryon charge of a single quark to be $1/N_c$, we find that

$$\boxed{Q_B = B.} \tag{143}$$

This confirms the conjecture that the winding number of skyrmions in our model is equivalent to baryon charge. Indeed, we have looked at properties of mass, radius and baryon charge, and these all seem to point towards the fact that the skyrmions in our field theory are in fact the baryons of QCD. This is a very exciting result, so let us now proceed in quantizing our theory, so that we can check whether other quantum numbers such as spin, isospin and hypercharge agree with what we would expect.

D.   Spin Statistics

This subsection is based on the chapter "Monopoles and Skyrmions" in Shifman [36].

As mentioned before in section III E, in order to interpret our skyrmions as baryons we need to overcome the issue of spin. Baryons are composed of three quarks and hence are fermions, whereas our field theory is purely mesonic, and hence spin 0. In order to properly reconcile this issue, we need to look carefully at the group structure of our theory. Recall that when we were discussing classical skyrmions in section III, we were working in the $SU(N_f = 2)$ group, corresponding to the up and the down quarks found in pions. In this section, when we seek to quantize the theory, we need to add more detail by making use of the Wess-Zumino term and so we work in $SU(N_f \geq 3)$. If we also consider the strange quark to be light, then it is natural to work in $SU(3)$ for most quantization purposes. It is important to note that even in this higher-order group, our previous results still hold. Namely, the hedgehog ansatz is still an energy minimiser in the Skyrme model for $B = 1$. However, we now think of the $SU(2)$ group that we were using as a subgroup of the full flavour group, $SU(N_f)$. For example, in this higher-order group space, the hedgehog ansatz may be written as

$$U_{\mathrm{H}} = \begin{pmatrix} \exp(iF(r)\hat{\boldsymbol{r}} \cdot \boldsymbol{\sigma}) & 0 \\ 0 & \mathbb{1}_{(N_f-2)\times(N_f-2)} \end{pmatrix}. \tag{144}$$

Aside: Surprisingly, D. Finkelstein and J. Rubinstein showed in 1968 that we can actually produce fermionic skyrmions in $SU(N_f = 2)$, without the Wess-Zumino term [37]. They exploited the fact that $\pi_4(SU(2)) \cong \mathbb{Z}_2$ and hence there are two topologically distinct classes of maps from space-time to $SU(2)$. Following from this, they weighted these two classes, so that one corresponds to a boson and the other to a fermion. However, due to the arguments presented in section IV A, this is generally not the correct way to quantize the theory and so is beyond the scope of this essay.

Instead, we look at our full action (including the Wess-Zumino correction) with fields in the full flavour group. We proceed by making a comparison between a skyrmion at rest and a slowly rotated skyrmion. We know that for a skyrmion at rest, all of the time derivatives in our Lagrangian density vanish and so the action may be written as

$$S_{\mathrm{rest}} = \int \mathrm{d}^3x\, \mathcal{L} \int_0^T \mathrm{d}t, \tag{145}$$

where we are looking at the skyrmion after some long time T. Recalling that for a static skyrmion, its energy, or equivalently its mass, M, may be written as

$$M = \int \mathrm{d}^3x\, (-\mathcal{L}), \tag{146}$$

we can express the action simply as $S_{\mathrm{rest}} = -MT$. Now, since in the path integral formulation the amplitude of a process is given by e^{iS}, we can deduce that the amplitude of a skyrmion at rest, after a long time, T, is given by e^{-iMT}.

Let us now compare this with the amplitude of a process where the skyrmion is slowly rotated by an angle of 2π. The motivation behind this step is of course the fact that fermions are spinors and so go to minus the identity after a 2π rotation. Conversely, bosons return to the identity after a 2π rotation. Therefore, by studying the 2π rotation carefully, we should be able to discern the criteria for the different skyrmion spin statistics. We consider a slow rotation (i.e. an adiabatic approximation), so that no other undesired physical effects come into play. With this in mind, we can see that the NLSM term along with the Skyrme term contain at least two time derivatives. The mass term, on the other hand, contains no time derivatives and so is of no interest to us. The crucial point to note is that the Wess-Zumino term, as presented (post Stokes' theorem) in equation 135, has four derivatives but five indices on its Levi-Civita tensor and so, overall it has one time derivative. In our adiabatic approximation, we are only interested in the terms that are leading-order in time derivatives and so, we can neglect the other terms in the action and focus only on the Wess-Zumino term. Recall now that the special feature of our hedgehog ansatz was that it showed an equivalence relation between rotations in real space and $SU(2)$ transformations. This is ideal for our current purposes as we would like to find a simple way of rotating by 2π in real space. Let us therefore rotate the hedgehog ansatz, such that

$$U'_{\mathrm{H}} = e^{(itT^3/2)}U_{\mathrm{H}}e^{-(itT^3/2)}, \qquad t \in [0, 2\pi), \tag{147}$$

where T^3 is the 3rd generator in the full flavour group $SU(N_f \geq 3)$ that forms an $SU(2)$ subgroup, since we have arbitrarily chosen to rotate in the 3-direction. By substituting this ansatz directly into the Wess-Zumino term, Witten showed that $\Gamma(U'_{\mathrm{H}}) = \pi$ [31]. Since we are only considering the Wess-Zumino term for time derivatives, the rotated action may be written as $S_{\mathrm{rot}} = S_{\mathrm{rest}} + N_c\Gamma(U'_{\mathrm{H}}) = -MT + N_c\pi$. The amplitude of this process may then be expressed as

$$e^{-iMT + iN_c\pi} = (-1)^{N_c}e^{-iMT}. \tag{148}$$

From this result, we can then see that the amplitude returns minus the identity when N_c is odd, and the identity when N_c is even. Since the hedgehog ansatz has this special equivalence between rotations in real space and $SU(2)$ group space transformations, we can conclude that

$$\begin{cases} N_c \text{ odd} & \Rightarrow \text{fermion,} \\ N_c \text{ even} & \Rightarrow \text{boson.} \end{cases} \qquad (149)$$

Furthermore, baryons are made up of three quarks of different colours, and so we conclude that the corresponding skyrmion is indeed a fermion. This argument is shown in greater detail in Witten's second paper on the subject [31].

E. Zero-mode Quantization

This subsection is based on the chapter "Monopoles and Skyrmions" in Shifman [36], the lectures by Gillioz [18] and the paper by Adkins, Nappi & Witten [28].

Now that we have built up our semi-classical theory of baryons and established their spin statistics, let us proceed by fully quantizing the model. There are many different ways of quantizing the theory at a variety of depths. In this section, let us look at the simplest possible quantization of rotation: the zero-modes around the $B = 1$ hedgehog skyrmion.

Zero-modes are the flat directions around our field solution and they will tell us information about the skyrmion at rest. In looking for the flat directions around the hedgehog solution, we look for its symmetries. Now the hedgehog ansatz trivially has a translation symmetry, however since we are only interested in quantizing rotation, this is of no interest to us. More importantly, the hedgehog ansatz has a symmetry under spatial rotations and $SU(2)_V$ transformations. Now in the special case of the hedgehog ansatz, we know that these two symmetries are equivalent. Therefore, they will both be significant to us as we try to quantize rotation.

Once we have established the applicable symmetries, we then introduce *collective coordinates* that parameterise these transformations. Let us denote our collective coordinates as $\theta_1(t)$, $\theta_2(t)$ and $\theta_3(t)$. Now if we allow our hedgehog skyrmion to rotate about all three spatial directions, we can then use the special property that spatial rotations are equivalent to $SU(2)_V$ transformations to express our new time-dependent hedgehog solution as

$$U_H(r, t) = R(t) U_H(r) R^\dagger(t), \qquad (150)$$

where

$$R(t) = e^{(i\theta_1 T^1/2)} e^{(i\theta_2 T^2/2)} e^{(i\theta_3 T^3/2)}. \qquad (151)$$

In this context, we can see that our collective coordinates may be thought of as Euler angles. In this discussion, we are ignoring the radial modes of the skyrmion as it rotates and all other such complications. The aim of this example is merely to demonstrate the simplest quantization procedure. If we now proceed by substituting our ansatz from

equation 150 into our full action (given in equation 133), we then find that

$$S = -M_H + \frac{1}{2} \Lambda_H (\dot{\theta}_i^2 + 2 \dot{\theta}_1 \dot{\theta}_3 \cos \theta_2), \qquad (152)$$

where M_H is the mass of the hedgehog skyrmion and Λ_H is its moment of inertia. The mass of the hedgehog skyrmion is the same as that calculated in section III E, and the moment of inertia is found to be

$$\Lambda_H = \frac{2\pi}{3} \frac{1}{f_\pi e^3} \int_0^\infty dr \, r^2 \sin^2 F \left(F'^2 + 1 + \frac{\sin^2 F}{r^2} \right). \qquad (153)$$

As before, this integral cannot be evaluated analytically. However, it is possible to find a numerical solution, which yields $\Lambda_H \approx 53.4/(f_\pi e^3)$ [18].

Now that we have an expression for the complete action in terms of our collective coordinates, we can proceed to quantize in the canonical way [38]. We can Legendre transform in terms of the canonical momenta, $\Theta_i = \dot{\theta}_i$, and subsequently make the operator promotion

$$\Theta_i \to i \frac{\partial}{\partial \theta_i}. \qquad (154)$$

By performing these two steps we find that our quantized Hamiltonian becomes

$$H = M_H + \frac{1}{2\Lambda_H} \left[\frac{1}{\sin^2 \theta_2} \left(\frac{\partial^2}{\partial \theta_1^2} + \frac{\partial^2}{\partial \theta_3^2} - 2 \cos \theta_2 \frac{\partial^2}{\partial \theta_1 \partial \theta_3} \right) \right. \\ \left. + \frac{1}{\sin \theta_2} \frac{\partial}{\partial \theta_2} \left(\sin \theta_2 \frac{\partial}{\partial \theta_2} \right) \right], \qquad (155)$$

which may be simply expressed as

$$H = M_H + \frac{1}{2\Lambda_H} \nabla_{S^3}^2, \qquad (156)$$

where $\nabla_{S^3}^2$ is the Laplacian on a 3-sphere, or equivalently the angular part of the 4-dimensional Laplacian. Fortunately, $\nabla_{S^3}^2$ is an eigenfunction and consequently so is the Hamiltonian. As we would expect from a spatial rotation operator, the Wigner D-functions, $D_{mm'}^j$, are its eigenfunctions [39] with the usual eigenvalues

$$\boxed{E_{mm'}^j = M_H + \frac{j(j+1)}{2\Lambda_H}.} \qquad (157)$$

Here $j \in \mathbb{Z} + \frac{1}{2}$ is the total angular momentum quantum number and m and m' are magnetic quantum numbers, which go from $-j$ to j in integer steps.

1. spin and isospin

Having found the eigenenergies of our system with respect to quantized rotations, the natural next step is look at the spin and isospin states. Recall that spin, J, and isospin, I, are defined as Noether charges associated with

rotations and isospin transformations, respectively. Applying Noether's theorem, using equation 150 in the full flavour group, we find that:

$$\begin{cases} J^k = -i\Lambda_{\mathrm{H}}\mathrm{tr}(R\partial_t R^\dagger T^k) & \text{spin,} \\ I^k = +i\Lambda_{\mathrm{H}}\mathrm{tr}(R\partial_t R^\dagger T^k) & \text{isospin.} \end{cases} \qquad (158)$$

where T^k are our full flavour group generators [18]. From this, we can see that for any skyrmion (since we have just used the Skyrme Lagrangian in calculating our Noether charges) spin and isospin are simply related by $SO(3)$ rotations. From this we can conclude that

$$J^2 = I^2, \qquad (159)$$

where J^2 is our squared angular momentum operator (and the only casimir of $SU(2)$). If we evaluate this operator in terms of our collective coordinates, we find that this is in fact equal to our Laplacian on the 3-sphere, $\nabla^2_{S^3}$. This allows us to write

$$H = M_{\mathrm{H}} + \frac{1}{2\Lambda_{\mathrm{H}}}J^2. \qquad (160)$$

Now we have simplified our quantized Hamiltonian to a constant term plus a term proportional to the squared angular momentum operator (which has the familiar eigenvalues of $j(j+1)$). We know that our physical states are eigenstates of the Hamiltonian and so correspond to the Wigner D-functions. We may denote them as

$$|j = i; m, m'\rangle, \qquad (161)$$

where i is the total angular momentum quantum number corresponding to isospin.

Note that for an even N_c, in the ground state there will be an equal number of quarks with spin up and spin down, and so the total spin of the particle will be zero. This implies that our particle is a *boson* with $j = 0$. Since the values of m and m' range from $-j$ to j in integer steps, we can see that there will only be one ground state, given by

$$|0; 0, 0\rangle. \qquad (162)$$

The case with an odd N_c, however, is more interesting. Generally, an odd N_c implies that our particle will be a *fermion* (as we saw in section IV D). In the ground state, the overall spin of our particle will be $j = 1/2$. Therefore, our ground state is now degenerate and may be given by

$$\left|\frac{1}{2}; \pm\frac{1}{2}, \pm\frac{1}{2}\right\rangle. \qquad (163)$$

Since baryons have an odd N_c, this will be our case of interest.

2. physical electric charge

Now adding electromagnetism to our theory involves moving from derivatives to covariant derivatives, $\partial_\mu U \to D_\mu U = \partial_\mu U - ieA_\mu[Q, U]$, and ensuring that our Wess-Zumino term is gauge invariant, $\Gamma \to \widetilde{\Gamma}$ [18]. As with a standard electromagnetism gauge theory, A is our vector potential and Q is our physical electric charge, given by the Gell-Mann-Nishijima formula,

$$Q = I_3 + \frac{1}{2}Y, \qquad (164)$$

where I_3 is the third component of the isospin and Y the hypercharge. Taking the third component of the isospin in equation 158, we find that

$$\widehat{I}_3 = \frac{1}{2}\Theta_1. \qquad (165)$$

If this operator acts on a state, we then find that

$$\widehat{I}_3 |i; m, m'\rangle = m |i; m, m'\rangle, \qquad (166)$$

which means that is has eigenvalues m. Now we saw in the previous section that for the N_c odd case (which corresponds to baryons), there are two possible values of m, that is $m = \pm 1/2$. This allows us to express our I_3 operator as a diagonal matrix:

$$\widehat{I}_3 = \begin{pmatrix} 1/2 & 0 \\ 0 & -1/2 \end{pmatrix}. \qquad (167)$$

In section IV C, we identified the baryon charge of individual quarks to be $1/N_c$. This, in fact, corresponds to the hypercharge generator, and in matrix form (for our N_c odd case) may be expressed as

$$\widehat{Y} = \frac{1}{N_c}\mathbb{1}. \qquad (168)$$

Hence, substituting these results into equation 164, we may write the physical electric charge operator for our fermionic ground state baryons as

$$\widehat{Q} = \begin{pmatrix} 1/2 & 0 \\ 0 & -1/2 \end{pmatrix} + \frac{1}{2N_c}\mathbb{1}. \qquad (169)$$

Now recall, from section IV C, that the baryon number symmetry corresponds to the $U(1)_V$ symmetry of our theory. Hence the $U(1)_V$ Noether charge corresponds to the hypercharge. By substitution of the $B = 1$ hedgehog ansatz and hypercharge generator into equation 139, we find that the hypercharge generator coefficient, $1/N_c$, cancels with the Wess-Zumino prefactor, N_c, and so

$$Y \equiv \int \mathrm{d}^3x\, J^0_Y = \frac{\cancel{N_c}}{\cancel{N_c}} = 1. \qquad (170)$$

This now allows us to calculate the physical electric charge of our particles. Note that if we had substituted the expression for the $B = -1$ skyrmion at this stage, we would obtain $Y = -1$, which would give us the charges for the corresponding antiparticles.

In this discussion, we only consider the fermion states, which correspond to baryons. Let us first consider the $|\frac{1}{2}; \frac{1}{2}, \frac{1}{2}\rangle$ state. We know that this state has an overall spin of $1/2$ and, from equation 164, we know that it has a physical electric charge of $+1$. Recall from section III E, that we estimated the hedgehog skyrmion mass

TABLE II. Candidate baryon particle states.

State	Mass / GeV	I_3	Spin	Charge / e	Particle
$\left|\frac{1}{2}; +\frac{1}{2}, +\frac{1}{2}\right\rangle$	~ 1	$+1/2$	$1/2$	$+1$	proton
$\left|\frac{1}{2}; +\frac{1}{2}, -\frac{1}{2}\right\rangle$	~ 1	$-1/2$	$1/2$	0	neutron

to be $M_{\mathrm{H}} \sim f_\pi/e \sim 1\,\mathrm{GeV}$. For any $j = 1/2$ configuration, we can see, from equation 157, that the skyrmion mass will now be given by

$$E_{\pm\frac{1}{2}\pm\frac{1}{2}}^{\frac{1}{2}} = M_{\mathrm{H}} + \frac{3}{8\Lambda_{\mathrm{H}}}. \tag{171}$$

At the start of this section, we estimated the moment of inertia to be given by $\Lambda_{\mathrm{H}} \sim 1/(f_\pi e^3) \sim 1\,\mathrm{MeV}\cdot\mathrm{fm}^2$ and so this shift in the energy is negligible. Hence the mass of our skyrmion state is still $\sim 1\,\mathrm{GeV}$. From the arguments discussed throughout this essay, we suspect that skyrmions in our field theory correspond to baryons. Here we have a baryon with a mass of the order of 1 GeV, an overall spin of $1/2$ and $I_3 = 1/2$, which implies a physical electric charge of $+1$. This corresponds to a *proton*.

Let us now consider the $\left|\frac{1}{2}; \frac{1}{2}, -\frac{1}{2}\right\rangle$ state. This state also has an overall spin of $1/2$, except this time with a different I_3 value. Hence, here we need to identify a baryon with a mass $\sim 1\,\mathrm{GeV}$, an overall spin of $1/2$ and $I_3 = -1/2$, which implies a physical electric charge of 0. This corresponds to a *neutron*. See table II, for a summary of our results.

V. MODELING LARGER NUCLEI

This subsection is based on the chapter "Skyrmions and Nuclei" by Battye, Manton & Sutcliffe [3].

In the previous section, we showed how, by quantizing the zero-modes around the hedgehog ansatz, the quantum states of the $B = 1$ skyrmion may be identified with the proton and the neutron - the building blocks of the nucleus. Following from this, it would be natural to now check whether skyrmions are able to model larger nuclei, so as to determine the theory's full range of applicability. Crucially, the Skyrme model can only be regarded as a *general* theory of nuclear structure if it is able to model *all* nuclei successfully. Let us proceed, therefore, by investigating the skyrmion solutions for larger baryon numbers, $B > 1$.

To begin, let us note a few important features of our treatment of the $B = 1$ skyrmion. In the $B = 1$ case, we used a 'spherically symmetric' hedgehog ansatz for the field configuration and showed that it is an energy-minimising solution of the Skyrme Lagrangian (see section III D). We used this to illustrate the massless pion field configuration, in real space, shown in figure 7. However, the hedgehog ansatz is not *generally* the energy-minimising solution of the Skyrme Lagrangian. In fact, it only minimises the field energy for $B = 1$. For higher baryon numbers, we need to use the rational map ansatz instead, as mentioned in section III E. The rational map ansatz, along with its extensions (e.g. the double rational map ansatz [40]), is suf-

FIG. 9. Baryon density isosurfaces, in real space, for $1 \le B \le 8$ skyrmions derived from massless pion fields. Each subfigure is labeled by its baryon number and symmetry group, respectively. [3]
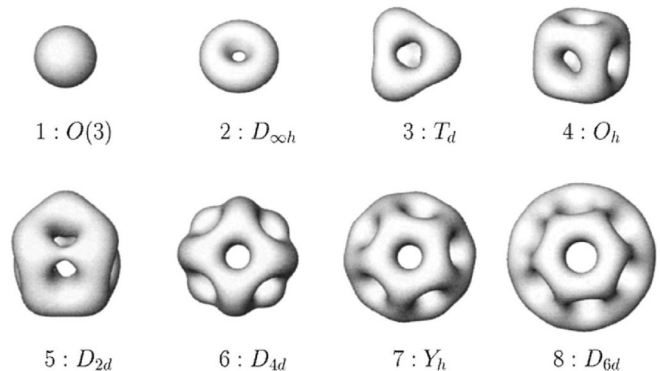
ficiently general to be successfully applied to many higher-order skyrmions [41]. Using a new energy-minimising field configuration is the first major change that we implement when moving to higher baryon numbers. Notice that this is a change in the *classical* treatment of the skyrmion, and so is made before any quantization takes place.

For the $B = 1$ skyrmion, we plotted the massless pion field configuration, in real space, and showed that it decays with separation from the origin in a spherically symmetric way (see figures 7 and 8). Therefore, if we were to plot a pion field isosurface, we would describe a sphere. Since our triplet of pion fields is being used to model a single baryon, this pion field isosurface corresponds directly to a baryon density isosurface, as shown in figure 9 - subfigure 1. Note that our chosen field configuration will always minimise the energy functional with respect to the winding/baryon number, and hence this correspondence is true in general. In this way, we are able to visualise the real structure of skyrmions. Illustrations of the first eight baryon density isosurfaces, using the single rational map ansatz, is shown in figure 9. Note that each isosurface possesses a high degree of symmetry, as we would expect from energy-minimising field configurations. The most stable (or energetically favourable) configuration in a classical system will usually show the highest degree of symmetry. In this case, the $B = 1$ hedgehog ansatz corresponds to one baryon and so has the lowest energy out of all the configurations, which explains why it is the most symmetric. The $B = 2, 3, 4$ states then show toroidal, tetrahedral and cubic symmetries, respectively. In fact, the $B = 4$ isosurface may be constructed from two $B = 2$ tori stacked on top of one another, along their common axis, with one of the tori flipped up-side down (as we shall explain in section V B). Similarly, the $B = 6$ skyrmion may be constructed from a stack of three $B = 2$ tori, with the middle torus flipped up-side down [42]. Continuing naïvely as in figure 9, using the single rational map ansatz, leads to all higher baryon number isosurfaces forming hollow polyhedra, reminiscent of carbon fullerenes [42]. As we shall discuss later, various problems arise when we deal with higher baryon numbers, $B \gtrsim 7$. For now, however, let us concentrate on the physical interpretation of the first few skyrmions.

A.   Deuteron ($B = 2$)

This subsection is based on the paper by Braaten & Carson [33].

The $B = 1$ skyrmion was the first skyrmion that was studied and initially proposed by Skyrme in 1961 [38]. This skyrmion solution was then quantized, using the conjecture that the winding number of the mesonic field theory may be interpreted as the baryon number, and hence that the $B = 1$ skyrmion corresponds to a single baryon. This theoretical exercise was successful, in that it predicted reasonable values for the quantum numbers and allowed Skyrme to identify the baryon as a proton or neutron [38]. However, without any proof to back up the conjecture, the logical progression to higher-order skyrmions remained unexplored for many years [33]. It was only in 1983, when Witten proved that this idea can be extended to $N_f \geq 3$ [30] and explained why fermions can arise from a bosonic field theory [31], that interest in this specific research was renewed. Following from this, in 1988, E. Braaten and L. Carson published a seminal paper on the $B = 2$ skyrmion, which they found possessed toroidal symmetry and upon quantization, they identified with deuteron (a proton-neutron pair) [33]. This paper then lead the way for many other attempts to model light nuclei, the majority of which have shown very good agreement with experimental results [43].

The simplicity of the $B = 1$ skyrmion lends itself to an intuitive physical interpretation. In the $B = 1$ case, we only have one baryon and so we would trivially expect the baryon density isosurface to be spherical; which is supported by empirical evidence [3]. However, the more unusual $B = 2$ toroidal skyrmion also has some phenomenological support [44]. Upon quantization, we deduce that deuteron has isospin 0 and spin 1 [42]. Deuteron is made up of a proton-neutron pair and so we would expect the baryon density to be of a familiar dumbbell shape. In fact, this toroidal skyrmion is consistent with our intuition. When the spin component along the z-axis is zero, the spatial wavefunction of deuteron (or any nucleon-nucleon pair) will be concentrated in a torus with the z-axis as its axis of symmetry, as confirmed by computational calculations [44]. However, if the spin component along the z-axis is ± 1, then the particle density would indeed take the shape of a dumbbell, as expected. This can be interpreted as a torus with its symmetry axis in the $x - y$ plane, spinning around the z-axis; and so our $B = 2$ skyrmion also has a consistent physical interpretation.

B.   The α-particle ($B = 4$)

This subsection is based on the paper by Battye, Manton & Sutcliffe [42].

The next two skyrmions, $B = 3$ and $B = 4$, are of particular significance because the corresponding particles are found to appear as substructures of larger nuclei. This is, in part, due to their highly symmetric, stable structure and ability to form bonds [41]. For this discussion, let us focus on the $B = 4$ cubic skyrmion. Upon quantization, this

TABLE III. The additive and subtractive primary colours along with their associated phase and unit vector. The colour spectrum is smooth and continuous, going from red back to red in the range $\phi \in [0, 2\pi]$. [41]

	red	yellow	green	cyan	blue	magenta
ϕ	0	$\pi/3$	$2\pi/3$	π	$4\pi/3$	$5\pi/3$
$\hat{\boldsymbol{\pi}}_1 + i\hat{\boldsymbol{\pi}}_2$	1	$\exp\left(i\frac{\pi}{3}\right)$	$\exp\left(i\frac{2\pi}{3}\right)$	-1	$\exp\left(i\frac{4\pi}{3}\right)$	$\exp\left(i\frac{5\pi}{3}\right)$

skyrmion may be identified with the helium nucleus (i.e. the α-particle) [42], which is made up of two neutrons and two protons.

The realisation that larger *skyrmions* can also be built out of $B = 4$ substructures is encouraging because it has been known since the 1930's, that many nuclei may be described as arrangements of α-particles (provided they have isospin 0 and B a multiple of four) [42]. As a consequence, it will prove to be a good investment to study the $B = 4$ skyrmion in more detail.

Let us start, however, by finding a more intuitive way to visualise skyrmion structure. The baryon density plots shown in figure 9 are undoubtedly a very useful way to visualise the overall shape of skyrmions. However, when it comes to skyrmion interactions, these plots do little to aid our understanding. For example, from figure 9, it is not obvious how two $B = 2$ tori may be combined to form a $B = 4$ skyrmion. In order to better visualise the skyrmion, we shall proceed by adding pion field phase information to the baryon density isosurfaces.

Consider the normalised pion field, $\hat{\boldsymbol{\pi}}$, given by

$$\hat{\boldsymbol{\pi}} = \frac{1}{|\boldsymbol{\pi}|} \begin{pmatrix} \pi_1 \\ \pi_2 \\ \pi_3 \end{pmatrix}. \tag{172}$$

In order to plot the pion field phase information on our baryon density isosurfaces, we shall use the *Runge colour sphere* convention. The Runge colour sphere, first introduced by P. O. Runge in 1810 [45], is a sphere which has the complete colour spectrum around its equator and transitions smoothly and evenly from 100% brightness (white) at the north pole to 0% brightness (black) at the south pole. The concept was first introduced to study colour in fine art, however it is useful in our context because it can encode a lot of information in a visual way. For the skyrmions, let us use the Runge colour sphere convention based on the $\hat{\boldsymbol{\pi}}_3$ component vector of the pion field. Let the south pole of the Runge colour sphere correspond to $\hat{\boldsymbol{\pi}}_3 = -1$ and the north pole to $\hat{\boldsymbol{\pi}}_3 = +1$. Since the colour sphere transitions smoothly and evenly, it follows that the equator corresponds to $\hat{\boldsymbol{\pi}}_3 = 0$. Now, for the colour spectrum, let us consider the argument of $\hat{\boldsymbol{\pi}}_1 + i\hat{\boldsymbol{\pi}}_2 = e^{i\phi}$ in the range $\phi \in [0, 2\pi]$. Let us define the phase plot to start at red for $\phi = 0$. The (additive and subtractive) primary colours along with their associated phase is shown in table III.

Recall that, in the case of the $B = 1$ hedgehog skyrmion, the pion field function shows a spherical symmetry. Therefore, plotting the pion field phase information onto the $B = 1$ baryon density isosurface produces the colour sphere itself, as shown in figure 10. Let us now interpret what

FIG. 10. Baryon density isosurfaces, in real space, for the $B = 1$ (hedgehog) and $B = 4$ skyrmions. The pion field phase is coloured using the Runge colour sphere convention. [41]
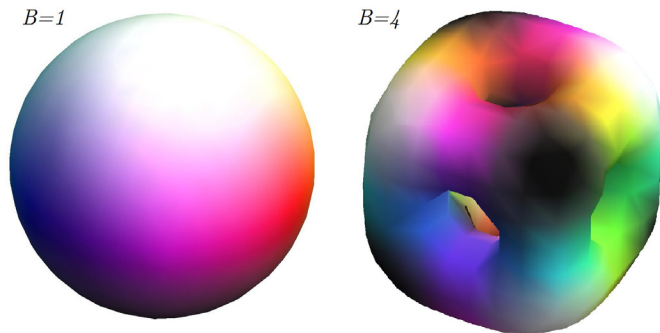
these colours are telling us about the physics of the situation. As we have shown in this essay, the Skyrme model is a *scalar* field theory and so the pion fields are scalar fields. This implies that charges/sources of equal sign will attract [41]. In this context, this refers to the pion field components. For example, the white section of the skyrmion with $\hat{\pi}_3 = -1$ will tend to be attracted to other white sections with $\hat{\pi}_3 = -1$ (as we shall see when discussing corner cutting in section V D). This gives us an easy way to visualise the construction of higher-order skyrmions, by bringing together smaller skyrmions and matching their colour at the joints. Going back to the example of constructing a $B = 4$ cubic skyrmion by 'gluing' together two $B = 2$ tori, we can now see why one of the tori must be flipped up-side down for this construction to work. Flipping one of the tori up-side down results in an attractive colour matching. Building on this, we may now plot the pion field phase information on the $B = 4$ cubic skyrmion, as shown in figure 10. This allows us to visualise how larger skyrmions may be constructed from these cubic building blocks.

Before we go on to construct larger skyrmions, however, we need to discuss the issues that we encounter when dealing with higher baryon numbers, $B \gtrsim 7$. There are three main problems with our current approach to constructing skyrmions, which only manifest themselves when modeling larger nuclei.

1. Volume scaling: Perhaps the most obvious problem with our current approach to skyrmion construction is the formation of large hollow polyhedra for higher baryon numbers, as we can see from the pattern emerging in figure 9. At the centre of these polyhedra, the energy and baryon density is very small, which implies that the nucleus is hollow. This clearly disagrees with what we have observed in real nuclei [42]. In smaller nuclei, such as $B = 2$ and $B = 6$, there is a physical interpretation as to why the nucleus can be empty at the centre, and this is supported by some empirical evidence [46]. However, for all other cases, we know that the baryon density should be approximately constant throughout the nucleus and scale $\propto B$. Our current skyrmion construction implies that the baryon density is confined to a

shell of approximately constant thickness, surrounding a cavity whose volume scales $\propto B^{3/2}$ [42]. This is in clear disagreement with experiment.

2. Spin/parity assignment: We have shown in section IV E, that when quantizing the $B = 1$ skyrmion we obtain quantum states with a spin/parity corresponding to real $B = 1$ particles. This is also successful for the $B = 2$ skyrmion, as well as other small skyrmions [42]. However, these quantum numbers are not consistent in general. Consider, for example, the $B = 7$ skyrmion shown in figure 9. This skyrmion shows a striking dodecahedral symmetry and seems to be a natural geometric progression from the lower-order skyrmion structures. However, upon (zero-mode) quantization, we find that the lowest spin state for isospin $1/2$ is spin $7/2$ [47, 48], which disagrees with experimental values of spin $3/2$ observed in the ground state of some $B = 7$ particles (namely, lithium and beryllium) [42]. This suggests that the highly symmetric structure that we have found for the $B = 7$ skyrmion may, in fact, be *too* symmetric to be the ground state solution. From a classical perspective, of course, this is undoubtedly the structure that minimises the classical energy. However, generally speaking, we could find a less symmetric structure, which has a larger classical energy but may be quantized with a lower spin, and so will yield a lower *total* energy. Therefore, it is not true, in general, that a structure that minimises the classical energy will also minimise the total energy, upon quantization. In fact, this tends not to be the case for higher baryon numbers.

3. Pion mass: Finally, the pion mass plays a significant role for higher baryon numbers [42]. Up to this point, we have mentioned the pion mass term (in section III E) but have since neglected it frequently, so as to benefit from the greater symmetry of a massless pion field theory. For example, all the skyrmions plotted in figure 9 are derived from a *massless* field theory. For small baryon numbers, this is indeed acceptable, as it has been shown that these solutions are relatively insensitive to the reduction in pion mass from its physical value to zero [49, 50]. However, for higher baryon numbers, we are no longer able to take this limit. For large hollow polyhedra, the addition of a pion mass term gives the centre of the skyrmion a field value of $U = -\mathbb{1}$, which is the antipode of the vacuum field value ($U = \mathbb{1}$). Therefore, these structures are highly unstable and tend to squash and pinch off into smaller sub-regions [42]. According to current research [50, 51], the qualitative properties of skyrmions are relatively insensitive to the actual (positive and non-zero) value of the pion mass and so it is common to take $m_\pi = 1$ for higher-order skyrmion simulations [41].

Taking these issues into account, let us now make some refinements to the way we model large skyrmions. First, let us include the pion mass term in our calculations with $m_\pi = 1$. Although more computationally intensive, this is

perhaps the simplest change to implement and will typically result in stable skyrmion structures. Second, we need to adopt, at least initially, a less systematic approach to constructing larger nuclei. Instead of blindly using the single rational map ansatz to build skyrmions that minimise the classical energy, we should treat each particle on a case-by-case basis and perhaps use what we already know about the geometry of the nuclear structure to efficiently find skyrmions that minimise the total energy after quantization. This should then solve both the volume scaling and spin/parity assignment issues.

Indeed, this is the approach that has been taken in recent years and to some degree of success [41]. For now, let us focus on nuclei that are built out of α-particles. We have known for many years that certain nuclei are composed of these building blocks. For example, beryllium-8, carbon-12 and oxygen-16 nuclei are made up of two, three and four α-particles, respectively [52]. This should give us some indication as to what skyrmion structures to expect when modeling these nuclei. For the purposes of this essay, let us focus on the possible nuclear configurations of carbon-12 for various energy states.

### C. The Hoyle State of Carbon ($B = 12$)

This subsection is based on the Physics World article by Jenkins & Kirsebom [52], as well as the papers by Lau & Manton [53] and Battye, Manton & Sutcliffe [42].

The states of carbon-12 are of particular interest to nuclear physicists because they clearly demonstrate gaps in our modern understanding of nuclear structure. Specifically, intensive research efforts have been focused around a particular state of carbon-12, known as the *Hoyle state*.

At the time of the big bang, we know that only three elements were produced: hydrogen, helium and (an extremely small proportion of) lithium. Heavier elements, such as carbon, are then produced through nuclear fusion in stars. Stellar nucleosynthesis predominantly involves four hydrogen nuclei (i.e. protons) fusing to form a helium nucleus (i.e. α-particle). Carbon is then formed when three of these α-particles fuse together at high temperatures. However, in order for three α-particles to join together, we first need two α-particles to join to form a beryllium-8 nucleus. This is where a problem occurs. Although two α-particles can indeed fuse to form a beryllium-8 nucleus, the nucleus is extremely short-lived with a lifetime of $\sim 10^{-16}\,$s [52]. Now, we know that all life on Earth is carbon-based and so carbon is relatively abundant. This extremely short lifetime of beryllium, however, would suggest that carbon has a very small probability of forming and cannot possibly account for the relative abundance that we observe today.

In 1953, British astrophysicist F. Hoyle reconciled this issue by postulating the existence of a short-lived excited state of carbon-12, now known as the Hoyle state, which would serve as a resonance and accelerate the production of carbon by seven orders of magnitude [54]. This excited state was postulated to have an excitation energy of $\approx 7\,$MeV and was experimentally confirmed to exist soon afterwards [55]. The theory proposed by Hoyle then suc-

FIG. 11. Configurations of carbon-12 based on the composition of three α-particles. (a) The earliest model of the Hoyle state, proposed in 1958, comprises a linear chain of three α-particles. (b) The ground state of carbon-12, or the most energetically favourable configuration of α-particles, is a compact triangular arrangement. (c) In 2001, it was suggested that the Hoyle state may be viewed as a Bose-Einstein condensate. (d) Most recently, in 2012, the Hoyle state was calculated from first principles and the α-particles were found to be in a bent arm configuration. [52]

a. linear chain

c. Bose-Einstein condensate

b. compact triangle

d. bent arm
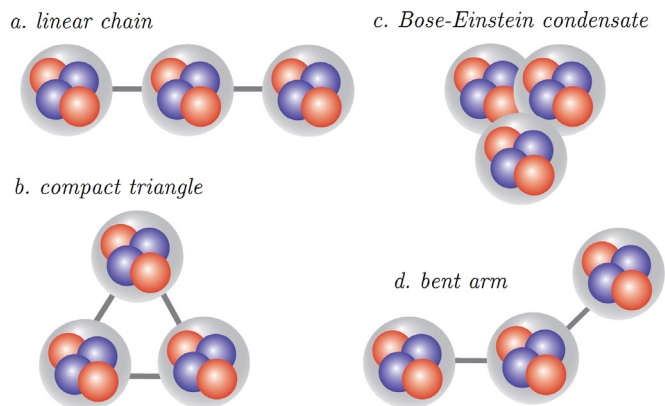
cessfully explains the relative abundance of carbon - a necessity for life on Earth. However, the current problem stands that the nuclear shell model, the best model of nuclear structure that we currently possess, does not predict the existence of such a state. In fact, similar short-lived excited states have now been observed in other light nuclei, which the model also fails to predict [52]. This demonstrates a major shortcoming in our understanding of the nucleus, and the topic is among the most intensely researched in the field of nuclear physics. It is interesting, therefore, to see what the Skyrme model has to say about the Hoyle state.

A few years after the discovery of the Hoyle state, it was proposed that instead of interpreting the carbon nucleus as a collection of independent nucleons, we interpret it as a cluster of three α-particles. The first model that was proposed was the linear chain, as shown in figure 11 - subfigure (a). Now this linear chain structure would be confined to a small nucleus length scale of $\sim 1\,$fm, and so, by Heisenberg's uncertainty principle, its momentum would be given a lower bound. At these expected energies, the α-particles could exchange nucleons between one-another, and so it was soon made apparent that a linear chain structure is a simplification which can only represent the time-average of a dynamic system [52]. However, this was a promising starting point and it inspired many new ideas. For example, since α-particles have spin 0, it was later suggested that the carbon-12 nucleus may, in fact, be a Bose-Einstein condensate, as depicted in figure 11 - subfigure (c). However, the consequences of such an idea were difficult to reconcile with our familiar understanding of the nucleus and so, it is not clear how this conjecture would fit in with our *general* nuclear model. Currently, the consensus is that the carbon-12 nucleus may actually be a superposition of states [52]. For example, the nucleus could be a 70% superposition of

FIG. 12. Baryon density isosurfaces, in real space, for the (a) linear chain (D_{4h} symmetry) and (b) compact triangle (D_{3h} symmetry) configurations of the $B = 12$ skyrmion. The skyrmions shown are derived from massive pion fields ($m_\pi = 1$) and the pion field phase is coloured using the Runge colour sphere convention. [53]

a. *b.*
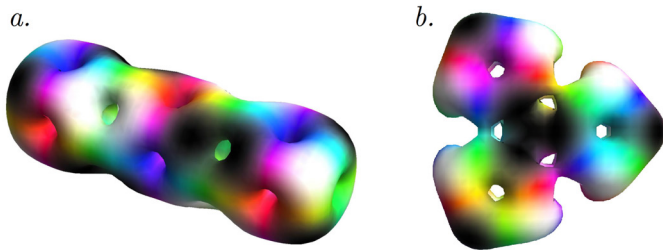
an α-particle cluster and a 30% superposition of a nucleon cluster. This way we can retain the key features of both models. However, this does not address the issue of what type of α-particle cluster could possibly be responsible for the Hoyle state.

In 2011, a theoretical physics group led by E. Epelbaum, from Ruhr-Universität Bochum in Germany, were the first to carry out an ab initio calculation of the energy states of carbon-12, using a Lattice Monte-Carlo simulation derived from QCD [56]. They indeed found a state at approximately 7 MeV above the ground state with spin 0 and positive parity (labeled 0^+), which can be identified as the Hoyle state. This was a promising result because a first-principles calculation can reveal the true structure of the nucleus. In 2012, they published a follow-up paper where they presented the nuclear structure that emerges from their simulations [57]. They found the ground state of carbon to be in a compact triangular arrangement of α-particles, as illustrated in figure 11 - subfigure (b). This result is intuitive because it possesses a high degree of symmetry. However, for the Hoyle state, they found that the nucleus was actually arranged in a bent arm configuration of α-particles, shown in figure 11 - subfigure (d). This is currently our best understanding of the Hoyle state and so, it begs the question: what are the total energy-minimising skyrmion structures for $B = 12$?

In 2014, P. H. C. Lau and N. S. Manton published a paper on "States of Carbon-12 in the Skyrme Model" to investigate this issue [53]. They found $B = 12$ skyrmion solutions to the Skyrme model numerically by allowing a symmetric arrangement of three $B = 4$ cubic skyrmions to relax to a minimal energy solution. The results showed two distinct skyrmion solutions, corresponding to the compact triangle and linear chain α-particle arrangements, as shown in figure 12. They then proceeded to quantize the rotational motion of these skyrmions and focus on the results for isospin 0. The results showed that the compact triangle configuration can be identified with the 0^+ ground state of carbon-12 (plus rotational excitations), and the linear chain configuration with the 0^+ Hoyle state (plus rotational excitations) [53]. The compact triangular ground state is in agreement with the results from QCD and is also somewhat intuitive. However, the linear chain 0^+ Hoyle

state seems to be in disagreement with the current bent arm consensus [57]. Furthermore, the skyrmion simulations were unable to confirm the ≈ 7 MeV excitation energy due to numerical uncertainties [53]. There are various possible explanations for this apparent disagreement. As we have mentioned before, the linear chain model is adequate as a time-averaged picture of a dynamical system. In fact, our current understanding is that the carbon-12 nucleus behaves rather like a gas of weakly-interacting α-particles that move almost freely on relatively large nuclear scales [52]. This allows us to take the time-average structure in this way. Moreover, it is known that the Skyrme model is built from an approximation to QCD and so, perhaps the results shown here are indeed in some time-averaged limit. In any case, it is interesting to see how the Skyrme model can be used to successfully (at least for the ground state) build nuclei out of $B = 4$ cubic blocks. There have been many detailed skyrmion calculations carried out for light nuclei built out of these cubes, which mainly show a very good agreement with experimental energies [41]. Given the success of building skyrmion structures out of cubes, compared to the large hollow polyhedra that we had earlier, it is now important to check the range of applicability of this new approach.

D. Higher Baryon Numbers

This subsection is based on the paper by Feist, Lau & Manton [41].

As we saw in section V B, simply applying the single rational map ansatz to all skyrmions does not work well for higher baryon numbers. A single rational map ansatz yields an incorrect volume scaling of the nucleus, as well as inconsistent spin/parity assignments for the ground state. Consequently, in order to reconcile this issue, we employ a multilayer rational map ansatz for larger nuclei [41]. The double rational map ansatz was the first to be considered [40], however many extensions exist. For example, the skyrmion structures shown in figure 12 were derived from a product map ansatz of particular arrangements of three $B = 4$ cubes. In this section, let us use the rational map ansatz that allows skyrmions to be geometrically constructed from the *Skyrme crystal* (as outlined in [41]) - the Skyrme crystal being an infinitely repeating (homogeneous and isotropic) structure made up of smaller skyrmion chunks. To begin our discussion, let us use the (special case) product map ansatz to produce an initial configuration and then, numerically relax the system to find an energy minimum. In particular, let us draw our attention to initial configurations made up of $B = 4$ cubic skyrmions.

After applying the product map ansatz to produce an initial configuration of $B = 4$ cubes and then numerically relaxing the system to obtain energy-minimising constructions, we find an impressive agreement with the ground state energies of a wide variety of large nuclei. For example, we find that the $B = 8, 24, 32$ skyrmions are made up of two, six and eight cubes, respectively [41]. Moreover, if we *do not* restrict ourselves to an initial configuration solely made of cubes and apply more general geo-

FIG. 13. Baryon density isosurfaces, in real space, for the $B = 108$ and $B = 100$ skyrmions. The skyrmions shown are derived from massive pion fields ($m_\pi = 1$) and the pion field phase is coloured using the Runge colour sphere convention. [41]

B=108   B=100
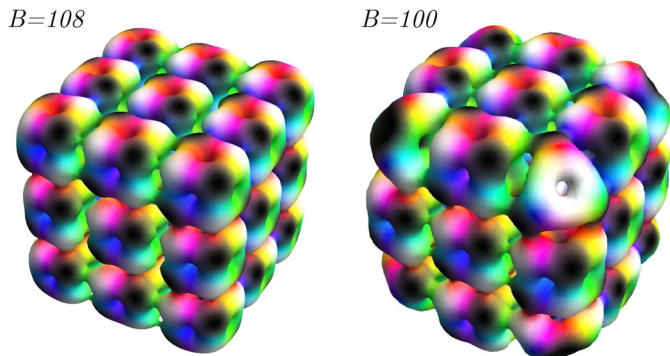
metric multilayer rational map ansätze, then we find that skyrmions 'naturally' tend to cluster into $B = 4$ subunits and some skyrmions can even be built up from a variety of building blocks. For example, the $B = 25$ skyrmion is built from a cluster of $B = 3$ tetrahedra and $B = 4$ cubes [41]. The largest skyrmion construction to show an agreement to real nuclear energies is, currently, the $B = 108$ skyrmion made up of twenty-seven $B = 4$ cubes using the three-layer rational map ansatz, as shown in figure 13. The construction clearly resembles a chunk of the Skyrme crystal. Note that one energetically-stable way of constructing lower-order skyrmions from larger structures is a method known as *corner cutting*. Recall that colour attraction in our diagrams means that white regions will be attracted to other white regions. Hence, at the corner of our larger cubic skyrmions, it is energetically stable to move the three white regions surrounding the corner into the corner black region to create a larger white region with a hole. Note that the concept of corner cutting is best understood in terms of geometric rational maps, which are beyond the scope of this essay [41]. In this way, we may remove corner baryons from larger cubic skyrmions to produce lower-order skyrmions. For example, we may remove the eight corner baryons from the $B = 108$ skyrmion to produce the $B = 100$ skyrmion, shown in figure 13. Alternatively, we could equally well modify the outer rational map by removing four corner baryons to produce a $B = 104$ skyrmion [41]. The corner cutting method was first introduced to derive the $24 \leq B \leq 31$ skyrmions from the large $B = 32$ cube (made up of four $B = 4$ cubes) [58]. It has since been shown to work well for many other baryon numbers [41].

VI. CONCLUSION

Starting from the sine-Gordon model in 1+1 dimensions, we have seen how field theories may have soliton solutions. These solutions must be both topologically stable, meaning that they have a non-trivial vacuum manifold topology, and energetically stable, meaning that they are local minima of the field energy. Skyrmions are solitons which have a non-trivial π_3 homotopy group and are found to be solutions to the NLSM - a rudimentary precursor to QCD. In order to make these topologically stable skyrmion solutions energetically stable, Skyrme added on the Skyrme term to the Lagrangian. One can then also add on a linear term to the Lagrangian to make the field theory massive. By considering a simple 'spherically symmetric' field ansatz, we then calculated the typical mass and RMS radius of a skyrmion which minimises the energy for a winding number of $B = 1$. We found that these values correspond well to the typical mass and size of some baryons. Adding on a third additional term to the NLSM Lagrangian allowed us to satisfy the CPT symmetry observed in nature and consequently, allowed us to quantize the theory. A simple rotation quantization of the $B = 1$ energy-minimising skyrmion, with the addition of electromagnetic gauge theory, allowed us to further calculate spin, isospin and physical electric charge. From this, we identified the skyrmions that correspond to the proton and the neutron. Building on this, we briefly reviewed attempts to construct higher-order skyrmions and discussed the complications that arise when trying to model larger nuclei.

This introduction to skyrmions in nuclear physics has demonstrated the profound results that can be drawn from this, seemingly basic, model of the nucleus. It allows us to interpret particles in a completely new way. Since its inception in the early 1960s skyrmions have found many applications to understanding nuclear structure [53], as well as applications to a wide variety of other fields of physics [3]. Most notably, magnetic skyrmions form a thriving area of research in condensed matter physics [59, 60]. However, the ideas of Skyrme have also found their way into more abstract physical theories, such as string theory [61]. Furthermore, as shown in chapter V, theorists have been able to find skyrmion correspondence with a large number of baryons, not only protons and neutrons. There has been a correspondence found with baryon numbers as high as $B = 108$ and all the energy-minimising solutions show a striking symmetry [41]. Theorists have even been able to study skyrmion scattering to better understand the particle scattering processes that experimentalists work with on a daily basis [62]. Undoubtedly, the study of skyrmions has provided us with a valuable insight, not only into the world of nuclear structure, but into physics as a whole. However, this area of research is by no means complete. The skyrmion correspondence between all baryon numbers has not yet been found, as certain particles, such a lithium-7 for example [42], are proving difficult to fit to the model. More importantly, skyrmions are solutions to the *effective* theory and not to the *fundamental* theory [18]. Hence, their full range of applicability and deep physical significance is yet to be precisely determined [18, 63].

[1] T. H. R. Skyrme, Proc. R. Soc. Lond. **A260**, 127 (1961).

[2] G. E. Brown, *Selected Papers, with Commentary, of Tony Hilton Royle Skyrme* (World Scientific, Singapore, 1995).

[3] G. E. Brown and M. Rho, *The Multifaceted Skyrmion* (World Scientific, Singapore, 2010).

[4] J. S. Russell, Brit. Assoc. Rep. **311** (1844).

[5] I. Newton, "Philosophiæ Naturalis Principia Mathematica," Book 2, London, UK (1687).

[6] D. Bernoulli, "Hydrodynamica," Strasbourg, France (1738).

[7] L. Rayleigh, Philos. Mag. 5, **1**, 257 (1878).

[8] D. J. Korteweg and G. de Vries, Philos. Mag. 5, **39**, 422 (1895).

[9] Image adapted from Wikipedia Commons (last accessed: 30/04/15).

[10] S. Demokritov, "Sine-Gordon Equation," Lecture notes (chapter 5), Münster University, Münster, Germany (2010), [last accessed: 30/04/15].

[11] Image adapted from Kyoto University On-line (last accessed: 30/04/15).

[12] Image adapted from Bochum University On-line (last accessed: 30/04/15).

[13] E. Bour, J. Ecole Imperiale Polytech. **19**, 1 (1862).

[14] Image adapted from Simon Fraser University On-line (last accessed: 30/04/15).

[15] Image adapted from Simon Fraser University On-line (last accessed: 30/04/15).

[16] R. J. Cova, in *The Sine-Gordon Model and its Applications*, Nonlinear Systems and Complexity (Springer, Cham, Switzerland, 2014) Chap. A Planar Skyrme-Like Model, p. 233.

[17] N. Manton and P. Sutcliffe, *Topological Solitons* (Cambridge University Press, Cambridge, UK, 2004).

[18] M. Gillioz, "An Introduction to Skyrmions," CP^3-Origins on-line lecture series, University of Southern Denmark, Odense, Denmark (2014), [last accessed: 30/04/15].

[19] G. H. Derrick, J. Math. Phys. **5**, 1252 (1964).

[20] E. Farhi, "An Introduction to the Skyrmion," Conference lecture, MIT, Cambridge, USA (1985).

[21] M. Gell-Mann and M. Levy, Il Nuovo Cimento **16**, 705 (1960).

[22] Image adapted from SlideShare South Korea (last accessed: 30/04/15).

[23] A. D. Jackson, in *Advances in Theoretical Physics: Proceedings of the Landau Birthday Symposium, 13-17 June 1988* (Pergamon Press, Oxford, UK, 1990) Chap. A Skyrmion Model of Two-dimensional Superconductors, p. 133.

[24] N. Riazzi, in *Theoretical Physics 2012: Part 1*, Horizons in World Physics (Nova Science, New York, USA, 2002) Chap. Geometry and Topology of Solitons, p. 133.

[25] M. Dunajski, Proc. Roy. Soc. Lond. **A469**, 20120576 (2013), arXiv:1206.0016.

[26] I. Zahed and G. Brown, Physics Reports **142**, 1 (1986).

[27] I. Floratos, *Multi-Skyrmion Solutions of a Sixth-Order Skyrme Model*, Ph.D. thesis, Durham University, Durham, UK (2001).

[28] G. Adkins, C. Nappi, and E. Witten, Nucl. Phys. **B228**, 552 (1983).

[29] A. Schmitt, in *Proceedings of the 16th Winter School "Geometry and Physics"* (Circolo Matematico di Palermo, 1997) pp. 147–151.

[30] E. Witten, Nucl. Phys. **B223**, 422 (1983).

[31] E. Witten, Nucl. Phys. **B223**, 433 (1983).

[32] S. Krusch, "Quantization of Skyrmions," (unpublished), University of Kent, Canterbury, UK (2006), arXiv:hep-th/0610176.

[33] E. Braaten and L. Carlson, Phys. Rev. **D38**, 3525 (1988).

[34] J. Wess and B. Zumino, Phys. Lett. **B37**, 95 (1971).

[35] Hence, $S_{WZ} \equiv \alpha\Gamma$ is often referred to as the Wess-Zumino-Witten term, as opposed to the Wess-Zumino term, Γ.

[36] M. Shifman, *Advanced Topics in Quantum Field Theory* (Cambridge University Press, Cambridge, UK, 2012).

[37] D. Finkelstein and J. Rubinstein, J. Math. Phys. **9**, 1762 (1968).

[38] T. H. R. Skyrme, Proc. R. Soc. Lond. **A262**, 237 (1961).

[39] J. Pagaran, S. Fritzsche, and G. Gaigalas, Comput. Phys. Commun. **174**, 616 (2006).

[40] N. S. Manton and B. M. Piette, Prog. Math. **201**, 469 (2001), arXiv:hep-th/0008110.

[41] D. T. J. Feist, P. H. C. Lau, and N. S. Manton, Phys. Rev. **D87**, 085034 (2013).

[42] R. Battye, N. S. Manton, and P. Sutcliffe, Proc. Roy. Soc. Lond. **A463**, 261 (2007), arXiv:hep-th/0605284.

[43] O. V. Manko, N. S. Manton, and S. W. Wood, Phys. Rev. **C76**, 055203 (2007), arXiv:0707.0868.

[44] J. Forest, V. Pandharipande, S. C. Pieper, R. B. Wiringa, R. Schiavilla, *et al.*, Phys. Rev. **C54**, 646 (1996), arXiv:nucl-th/9603035.

[45] P. O. Runge, "Die Farben-Kugel, oder Construction des Verhältnisses aller Farben zueinander," Hamburg: Perthes, Germany (1810).

[46] G. S. Anagnostatos, A. N. Antonov, P. Ginis, J. Giapitzakis, and M. K. Gaidarov, J. Phys. **G25**, 69 (1999).

[47] P. Irwin, Phys. Rev. **D61**, 114024 (2000), arXiv:hep-th/9804142.

[48] S. Krusch, Ann. Phys. **304**, 103 (2003), arXiv:hep-th/0210310.

[49] R. Battye and P. Sutcliffe, Nucl. Phys. **B705**, 384 (2005), arXiv:hep-ph/0410157.

[50] C. Houghton and S. Magee, Europhys. Lett. **77**, 11001 (2007), arXiv:hep-th/0602227.

[51] R. Battye and P. Sutcliffe, Phys. Rev. **C73**, 055205 (2006), arXiv:hep-th/0602220.

[52] D. Jenkins and O. Kirsebom, "The Secret of Life," Physics World, February, 23 (2013).

[53] P. H. C. Lau and N. S. Manton, Phys. Rev. Lett. **113**, 232503 (2014), arXiv:1408.6680.

[54] F. Hoyle, Astrophys. J. Suppl. S. **1**, 121 (1954).

[55] E. M. Burbidge, G. R. Burbidge, W. A. Fowler, and F. Hoyle, Rev. Mod. Phys. **29**, 547 (1957).

[56] E. Epelbaum, H. Krebs, D. Lee, and U.-G. Meißner, Phys. Rev. Lett. **106**, 192501 (2011), arXiv:1101.2547.

[57] E. Epelbaum, H. Krebs, T. A. Lähde, D. Lee, and U.-G. Meißner, Phys. Rev. Lett. **109**, 252501 (2012).

[58] N. Manton, Math. Method. Appl. Sci. **35**, 1188 (2012).

[59] S. Girvin, Physics Today **53**, 39 (2000).

[60] C. Schütte, *Skyrmions in Chiral Magnets*, Ph.D. thesis, Cologne University, Cologne, Germany (2014).

[61] P. Sutcliffe, J. High Energy Phys. **1008**, 019 (2010), arXiv:1003.0023.

[62] N. S. Manton, Phys. Rev. Lett. **60**, 1916 (1988).

[63] S. M. H. Wong, "What exactly is a Skyrmion?" (unpublished), The Ohio State University, Columbus, USA (2002), arXiv:hep-ph/0202250.